Small-Scale Heterogeneity in Sediments: Experimental and Modelling Investigations

Anthony Stockdale MChem

August 2008

This Thesis is Submitted for the Degree of Doctor of Philosophy.

Acknowledgements

I am indebted to my supervisor Bill Davison who first encouraged me to apply for the project. Bill and my co-supervisor Hao Zhang provided support, advice and encouragement throughout the practical and writing stages of the thesis. I believe that often, ideas are best discussed as soon as possible after their conception so they are not lost to the ether. In this respect, Bill was a model supervisor as he was always available for a chat to help solidify my latest ideas, thanks Bill.

Several additional members of the Environmental Science Department deserve recognition: group technician Debbie Hurst who provided much assistance (not to mention having to do all of the driving) when sediment sampling at Fleetwood and Esthwaite Water; Kent Warnken who provided training on use of the laser ablation instrument; and John Hamilton-Taylor who was the chair of my supervisory panel.

Thanks to the Freshwater Biology Association for use of the boat facilities at Esthwaite Water and to the Port of Fleetwood for permission to collect samples from Fleetwood Marina.

I am grateful to those fellow scientists who provided data, figures or information, and those who gave permission for figures to be reproduced: Joan Bernhard, Suzanne Dufour, Les Watling, Frank Wenzhöfer and Quinzhi Zhu for figures in Paper I; Peter Berg who provided data for some modelling that ultimately was not used; Anders Widerlund who provided clarification of gel drying procedures and source data to calculate microniche size distributions from a published figure; Bernie Boudreau who replied to a query about model validation procedures and Ronnie Glud who answered a query on the effect of planar optodes on diffusion for Paper I. Special thanks go to Bob Aller for a very thorough reviewing effort which led to significant improvements to Paper I, in particular my appreciation of historical concepts in sediment heterogeneity would be much poorer without his effort.

List of papers

I.   Stockdale, A., Davison, W., Zhang, H., (Peer reviewed and revisions submitted). Micro-scale biogeochemical heterogeneity in sediments: A review of available techniques and observed evidence. Earth-Science Reviews.

II.   Stockdale, A., Davison, W., Zhang, H., 2008. High-resolution two-dimensional quantitative analysis of phosphorus, vanadium and arsenic, and qualitative analysis of sulfide, in a freshwater sediment. Environmental Chemistry, 5, 143-149. DOI: 10.1071/EN07096

III.   Stockdale, A., Davison, W., Zhang, H. Quantifying cobalt fractions associated with iron and manganese (oxyhydr)oxides in marine sediment using DGT.

IV.   Sochaczewski, Ł., Stockdale, A., Davison, W., Tych, W., Zhang, H., 2008. A three-dimensional reactive transport model for sediments, incorporating microniches. Environmental Chemistry, 5, 218-225. DOI:10.1071/EN08006

V.   Stockdale, A., Davison, W., Zhang, H. Sulphide evolution from faecal pellets and other microniches within sub oxic surface sediment: The effects on the geochemistry of iron and trace elements. Submitted to Geochimica et Cosmochimica Acta.

Small-Scale Heterogeneity in Sediments: Experimental and Modelling Investigations

Anthony Stockdale MChem

August 2008: This Thesis is Submitted for the Degree of Doctor of Philosophy.

Abstract

This thesis consists of several studies relating to small-scale heterogeneity in sediments. The principal aim was to further our understanding of processes occurring at microniches. The individual studies consist of: 1) a critical review of previous studies of microniches that used probes with high spatial resolution and modelling approaches; 2) an experimental study of analysis of oxyanions in sediment at high resolution that applied a newly developed preparation method for a combined AgI/FeOOH binding phase, to investigating processes occurring at a sulphidic microniche within a freshwater sediment; 3) analysis of the relationship between trace metal (cobalt) and iron and manganese in a marine sediment using DGT, although this is not directly related to microniches, these data are useful in modelling the release of microniche trace metal from authigenic oxides; 4) the development and application of a three-dimensional diagenetic model to investigate conceptually the geochemical behaviour of microniches under different conditions, and to interpret modelled observations in terms of data from the literature and known trace element geochemistry. The key results/conclusions from both the laboratory and modelling studies are: 1) for a freshwater sediment, depletions in anions (of P, V, As) at a microniche of elevated sulphide were observed and the behaviour of phosphate at this niche was attributed to uptake associated with elevated activity of sulphate reducing bacteria; 2) modelled scenarios, with varying microniche properties, were shown to be relevant to experimental observations reported in the literature. The preferential deposition of FeS at the edge of microniches (with lifetimes of 2.5-5 days), forming 'crustal' deposits was demonstrated. The modelled data indicated that microniches may be significant in terms of the formation of some trace element sulphides. This thesis also contains an assessment of the significance of microniche processes and a discussion of priorities for future work.

Contents

Contents of Papers

(Section numbering is included where it is an integral part of the Journal's format)

Paper II: High-resolution two-dimensional quantitative analysis of phosphorus, vanadium and arsenic, and qualitative analysis of sulfide, in a freshwater sediment

Environmental context

Abstract

Introduction

Principles of DGT

Materials and Methods

Preparation of diffusive gel

Preparation of the combined AgI-FeOOH binding layer

Preparing the AgI phase

Addition of the iron oxide phase

Calibration procedure

Deployment procedure

Laser ablation procedure

Obtaining qualitative sulfide data

Results and discussion

Analytical performance

In situ profiles

Conclusions

Acknowledgements

References

Accessory Materials

Gel drying procedure

Laser ablation TRA data processing procedure

Paper III: Quantifying cobalt fractions associated with iron and manganese (oxyhydr)oxides in marine sediment using DGT

Abstract

1.   Introduction

2.   Materials and Methods

2.1.   Sampling and experimental setup

2.2.   DGT preparation and deployment

2.3.   Experimental and sample processing procedures

2.4.   Data analysis

3.   Results and discussion

3.1.   Effects of sediment ageing and general observations from the profiles

3.2.   Comparison of the Fe, Mn and Co data

4.   Conclusions

Acknowledgements

References

Paper IV: A three-dimensional reactive transport model for sediments, incorporating microniches

Environmental context

Abstract

Introduction

Modelling of microniches

Microniche sources and life-span

Aims and approach

Model formulation

Model inputs and calculations

Modelling solute dynamics at microniches of varying size

Conclusions

Acknowledgements

References

Accessory Materials

The graphical user interface (GUI)

Model output

Resolution explained

Further details on mesh implementation

Model implementation

Additional options for microniche specification

Example equation for validation procedure

Tortuosity options in 3D-TREAD

Data used as model input parameters

Paper V: Sulphide evolution from faecal pellets and other microniches within sub oxic surface sediment: The effects on the geochemistry of iron and trace elements

Abstract

1.   Introduction

1.1.   Trace element/sulphide geochemistry

1.2.   Geochemistry of microniches

1.3.   Modelling of microniches

1.4.   Aims and rationale of this work

2.   Modelling framework

2.1.   Model description

2.2.   Setup of model simulations

2.3.   Treatment of iron-sulphide reactions

3.   Results and discussion

3.1.   Description of modelled scenarios

3.2.   Iron and sulphide at microniches

3.2.1.   Trends related to porosity and rate

Figures

Paper I

1.	Schematic of the effect of scaling on porosity observations

2.	Intact faecal pellets observed by slicing of a resin embedded sediment

3.	Comparison of the sediment total oxygen uptake ratio (ex-situ/in-situ) against the depth of overlying water

4.	In situ microelectrode oxygen profile for an Atlantic Ocean sediment

5.	Example data from (pH) planar optodes

6.	High-resolution DGT derived data

7.	Data visualisations available from colourimetric probes

8.	2D data from x-ray tomography and life positions studies

Paper II

1.	Time series of counts (cps) recorded by the ICP-MS

2.	2-D high-resolution V, As and P profiles at a sulphidic microniche

Paper III

1.	Co, Mn and Fe DGT concentration profiles (C_{DGT}) from intact sediment cores

2.	Co, Mn and Fe DGT concentration profiles (C_{DGT}) from aged sediment

Paper IV

1.	Illustration in 2-D of the approximation involved in representing a circular microniche (circle) by a FEM mesh of triangles

2.	Vertical porewater profiles at the microniche centres

3.	Comparisons of vertical O_2, NO_3^-, and ΣS(-II) profiles at the 3.75 mm microniche and profiles when no microniches are present

4.	Time series of solute profiles within a microniche

5.	Contour plots of sulphide concentrations through a microniche

S.1.	User interface for 3D-TREAD

S.2.	Example calculation for validation procedure

S.3.	Initial profile inputs for the microniche modelling

Paper V

1. Degree of trace metal pyritization vs. degree of pyritization

2. Relationship between organic carbon decomposition rate, porosity and microniche lifespan

3. Concentrations of sulphide, iron and the related saturation index

4. 2D representation of $\sum S(-II)$, Fe(II) and FeS concentrations after a 24 hour model run, and a schematic of FeS deposition at microniches

5. FeS concentrations after a 24 hour model run

Tables

1   Introduction

Thesis regulations state that the introductory chapter should cover 'the whole of the background and context of the research.' However, this thesis includes, as an independent chapter, a substantial critical literature review covering a large part of the background and context to this work (Paper I). In order to avoid unnecessary repetition, I have written the introduction so that it complements, rather than repeats, Paper I. The introduction includes those subjects that are absent from the review chapter. These topics are, a description of the characteristics of microniches and their location and a review of the modelling of microniches. Additional to the thesis requirements, an assessment of the wider significance of microniche processes is included, following the thesis conclusions.

1.1   Definitions of microenvironment and microniche

Despite the fact that these terms are defined elsewhere in the thesis, it is important to define these from the outset. I define a microenvironment as a localized location within the 3-dimensional sediment matrix where the geochemistry is significantly different from the average for that depth. This may apply to a gas bubble, a burrow or feeding tube from a benthic organism, or a particle of reactive organic matter or other component that has biogeochemical reaction rates that are higher than the surrounding environment. The term microniche is reserved for microenvironments associated with localized reactive organic matter.

1.2   Description of thesis structure

This thesis is composed of five papers related to trace metal and microniche geochemistry. A comprehensive critical literature review (Paper I), practical studies

(Papers II and III) and modelling studies (Papers IV and V) form the basis of this thesis. Descriptions of these papers are included in Section 3.

1.3 The characteristics of microniches and their surroundings

1.3.1 Environmental conditions around microniches

The physical and chemical characteristics of a sediment will have a large effect on determining the significance of microniches in different deposition environments. Table 1 shows different sediment and microniche characteristics and their potential effect on sulphide production or long-term effects. As is evident from the scenarios in Table 1, size, rate and porosity have the greatest influence on the potential for niche sulphide evolution in the O_2/NO_3^- zones. Below these zones these characteristics exert less influence. For microniches to have any long-term effect on sediment geochemistry, such as the formation of trace element-sulphides, the relative reversibility of such formation is an important consideration. For a niche where trace element-sulphides have formed, to have any long-term effect on element accumulation, the effects must not be fully reversible. Cyclical processes such as re-suspension may negate microniche effects by stimulating reoxidation of reduced species within niches. Overturn by biota may have the greatest influence on long-term effects, as these processes are important in introducing niches to various depths. Conversely, it may also relocate degraded niches to a zone where they are subject to re-oxidation (resulting in an oscillating redox condition). The degree of reversibility of formation reactions will influence the degree to which this reoxidation process affects different elements. For example, ZnS is oxidised more slowly than FeS (e.g. Sukola et al, 2005), and the oxidation of tetrathiomolybdate to molybdate has a slow rate (Erickson and Helz, 2000). Tetrathiomolybdate is also more readily scavenged by

Table 1. Effect of microniche and sediment characteristics on sulphide production and/or long-term effects. Scenarios assume sulphate availability within the sediment.

Characteristic	Scenario and effect
Microniche	
Size (volume)	The larger the niches the greater the likelihood of sulphide production within the oxic and suboxic zones.
Organic matter reaction rates	The greater the rate the greater likelihood of sulphide production within the oxic and suboxic zones. Increased rates will tend to increase peak sulphide concentrations and decrease the life-span of the niche. The contrast between the OM reduction rates in the 'bulk' sediment and the microniche will be important in assessing the significance of the niche.
Authigenic oxide concentration	Authigenic oxides will provide an alternative electron acceptor and sulphide will not evolve until these oxides are below their limiting concentration. Authigenic oxides may yield significantly higher trace metal evolution than OM alone. The relative ratios of oxides to available niche organic matter will control if sulphate reduction occurs within a niche.
Porosity	Within the oxygen and nitrate decomposition zones a high porosity niche will tend to require either a large size, high OM degradation rates or a combination of both factors, before sulphate is consumed. The lower the porosity of the niche the greater the sulphate production (providing the rate constant is equal). If the niche porosity is different from the bulk value, diffusion coefficients will differ within each zone and this may have an effect on the rates of resupply required to maintain e.g. iron sulphide precipitation.
Diffusional barriers (e.g. peritrophic membranes or hard parts)	The presence of a peritrophic membrane or hard parts (such as a shell) may restrict diffusion into or from the niche. This may lead to a more rapid consumption of oxygen and nitrate, resulting in sulphate reduction. All oxidants may be consumed.
Sediment	
Redox oscillations	Where sediment overturn via bioturbation is significant, redox oscillations may occur. Any formation of trace element-sulphides at microniches may be fully reversed by oxidation. Whilst bioturbation is important in the formation and distribution of microniches, the extent to which this process reverses the formation of sulphides also needs to be considered.
Microniche depth	When present in the sulphate reducing zone, microniches will produce zones of elevated sulphide regardless of their size. If they contain authigenic oxides, localised formation of metal sulphides may be expected. Sulphidic niches within the manganese and iron oxide reducing zones may result in net diffusion of trace elements into the niche with subsequent localised precipitation of sulphides.
Redox conditions above sediment-water interface	Where overlying water is permanently anoxic, bioturbation may by limited. Microniche sources will be limited to settling material, and sulphate reduction is likely to proceed in the water column before the particle settles. In such an environment, redox conditions of the niche will not significantly differ from the surroundings and the long-term effect of localised zones may be minimal.
Oxygen and nitrate penetration depth	Niches within the oxic and NO_3^- zones require either a large size, high OM degradation rates, limited diffusion (membranes) or a combination of such processes, before sulphate is consumed. Niches within the oxygen and nitrate zones may have discrete layers oxidised by different oxidants. Niches present below the nitrate penetration depth will require physical movement into oxic and NO_3^- zones for reverse redox processes to occur.
Organic matter concentration	In pristine or low OM environments, oxygen will tend to be present at much greater depths than more productive sediments. In such environments any formation of trace-element sulphides will tend to be reversible as, after the niche is consumed, oxygen is readily available.
Cyclical processes	Numerous processes may apply to this category. Some examples are given. Productivity and thus microniche creation may vary with seasons. In marine tidal regions, cyclical processes such as, tidal forcing (advection) and sediment re-suspension may occur. In lakes, seasonal variations in stratification may have effects on the sediment redox conditions.

FeS$_2$ and FeS than molybdate, further slowing its oxidation (Bostick et al, 2003; Helz et al, 2004).

1.3.2   Properties and types of microniches

As the term microniche applies to any discrete site of reactive OM, this can encompass material from a range of different sources. Microniches can be attributed to decaying organisms (observed using a pH optode; Zhu et al, 2006), algal aggregates (added to sediment to study sulphidic microniches; Widerlund and Davison, 2007) and faecal pellets (photographed after resin embedding and thin sectioning of an intact core; Watling, 1988). Within vegetated sediments such as mangroves, root systems can also generate microniches (e.g. Alongi et al, 2004). Such niches will have a range of different properties. For example: algal aggregates will tend to have a high porosity and a low concentration of authigenic oxides; faecal pellets may possess a peritrophic membrane, be more compact than the ambient sediment (lower porosity) and in some cases have been shown to contain a greater distribution of fine mineral grains than the ambient sediment (Watling, 1988), potentially affecting tortuosity.

Jørgensen (1977) estimated a detrital particle scale range of one µm to several millimetres or centimetres. Johnson (1974) examined the particle components of a surface sediment, including the consideration of particles that may be potential sources of food and thus may potentially produce microniches. Potential food sources such as diatoms, algae and pollen/spores had sizes as low as 5-85 µm, with the upper size range being ~1000 µm for diatom and algal chains. Faecal pellets ranged from 10 to 650 µm diameter, the upper value being consistent with observations by Watling (1998), who observed cylindrical pellets with widths of approximately 200 µm and

lengths ~500 µm. Taghon et al (1984) observed faecal pellets from a tube dwelling marine polychaete (*Amphicteis scaphobranchiata*) with an approximate average size of six mm length and one mm width. For cylindrical faecal pellets, width will be the most important factor for the formation of microniches as the shortest diffusive path will be the controlling factor for the resupply of oxidative solutes to the centre of the niche.

For small particles, such as those observed by Johnson (1974), to form as microniches, specific conditions must be met: 1) they must occur below the depth where oxygen and nitrate are both below the concentration at which, less energetically favourable oxidants are utilised to degrade organic matter, 2) where they contain authigenic oxides (e.g. in the case of some faecal pellets) the concentration of these components must be limited compared to the available OM, and/or, 3) they must be present in the sulphate reducing zone. Widerlund and Davison (2007) used diffusive gradients in thin-films (DGT) and computer imaging densitometry (CID) to quantify microniche sulphide distributions in a sulphidic freshwater lake sediment. A majority of the observed niches (~62%) were in the size range of 0.8 to 1.6 mm diameter, assuming spherical geometry (actual modal circularity value was 0.9). Microniches with a diameter above 2.5 mm accounted for ~12% of the total number of niches. Despite their lower numbers compared to smaller niches such microniches can occupy a relatively large volume (e.g. a 2.5 mm diameter niche has a volume equal to 125 individual 0.5 mm niches, assuming spherical geometry).

In terms of depth distributions, Johnson (1974) found that non-algal plant fragments showed no significant difference in abundance between the surface (sediment-water

interface) and two centimetres depth sediment samples. Faecal pellet abundance was approximately one third less at two cm depth, with the most significant difference being in the abundance of micro-algae, which at two cm depth was ~16% of the surface abundance. When all potential food particles are considered as a single group (this includes organic-mineral aggregates), there was no significant difference in abundance between the surface and two cm depth samples.

1.3.3   Settling particle microniches (faecal pellets and marine snow)

Settling particles within the water column such as faecal pellets and aggregates (termed marine snow), have been identified as localized zones of heterotrophic activity within the water column. When these particles settle on the sediment surface and are introduced into the sediment by the actions of biota they may form microniches. In situ metal deposition may occur within settling particles during passage through the water column, via precipitation of metals within extracellular capsules of bacteria. This may have an impact on water column chemistry (Cowen and Silver, 1984) and provide increased levels of reactive metals if such particles ultimately form sediment microniches. Settling particles are, by their nature, more readily identifiable than sedimentary microniches and have been studied directly, providing evidence for the existence of reducing micro-zones, and the processes occurring within them. The particle sizes observed for marine snow vary greatly from <100 µm to several decimetres in diameter (Hamner et al, 1975). Marine snow can have microbial communities with densities several orders of magnitude higher than in surrounding seawater (Alldredge et al, 1986). Zooplankton faecal pellets have been measured to sink at rates between 15 and 950 m per day (Cherry et al, 1978; Alldredge, 1979 and references therein).

The chemistry of both marine snow and faecal pellets has been investigated using microelectrodes. A faecal pellet attached to a particle of marine snow was shown to have a significantly larger number of bacteria per volume than a marine snow particle, with the same pellet undergoing a pH decline of up to 0.91 units, and complete oxygen depletion during dark conditions (Alldredge and Cohen, 1987). This study also observed oxygen depletions of up to ~46%, and a lowering of pH by 0.22 units (compared to surrounding water), in a marine snow particle of 4.1 mm diameter. For a microniche within a marine sediment Ploug et al (1997) observed oxygen depletion, and a lowering of the pH from 8.2 in the ambient sediment to 7.4, in the centre of an anoxic aggregate (1.4 mm diameter). Sulphide was not analysed in these studies.

The potential for marine snow to produce sulphide within a seawater with a low oxygen concentration was examined by Shanks and Reeder (1993). Using tetrazolium salts, and both artificial and field samples of marine snow, they showed that sulphide evolves in aggregates of 0.7 to 2.0 mm in diameter. Within pieces of detritus (such as diatom frustules), elevated concentrations of sulphide were detected. This was attributed to a reduced flux of O_2 into these zones, caused by the physical structure of the detritus. Within sediments larger examples of microniches within shell structures have been observed within the oxic and suboxic zones (e.g. Emery and Rittenberg, 1952).

In comparison to sedimentary microniches, settling particle microenvironments will tend to have higher ambient surrounding concentrations of oxygen, and advective flow of fluid around the particle as it sinks may aid solute transport (although, Alldredge and Cohen, 1987; observed that boundary layers hundreds of micrometers thick are

maintained despite this advection). Within sediments, because of reduced transport and higher bacterial populations, the conditions required for microniche formation are optimised compared to the water column. The extent to which sinking particles have an effect on microniche formation in sediments will depend upon whether they reach the sediment while they are still metabolically active.

The direct study of marine snow microniches has provided useful insights into the geochemistry of isolated reactive particles. However, this work has seldom been recognised by those investigating microniches. Changes in pH observed in 1D for marine snow using electrodes (Alldredge and Cohen, 1987; Ploug et al, 1997) have been confirmed for microniches in 2D using planar optodes (Zhu et al, 2006). Sulphide production within marine snow was identified in very small (0.7-2 mm) aggregates of reactive matter (Shanks and Reeder, 1993), before being reported in 2D at high resolution within sediments (Devries and Wang, 2003). From these studies we can conclude that there is some common geochemistry shared by the particles in the different environments. Direct analysis of marine snow particles is more easily achieved than direct study of microniches and this provides an opportunity to use the full range of electrode probes (listed in Paper I) to further our geochemical knowledge of microniches for a range of elements or species.

1.4   Modelling of microniches

The modelling of microniches was pioneered by Jørgensen (1977), who investigated the conditions required for the presence of oxygen depletion within microniches in the oxic zone of the sediment. Adopting a 1D approach, the O_2 consumption was modelled, considering microniche size (diameter, spherical geometry was adopted)

and ambient O_2 concentrations. Jørgensen (1977) calculated that for anoxia to occur at the centre, a niche would have to be two millimetres in diameter when the O_2 concentrations were that of saturated seawater and the respiration rates within the niche was five times the sediment average (a very conservative estimate). At 1% O_2 saturation the minimum niche diameter required was 200 μm.

Jahnke (1985) recognised that microniches rich in organic matter may support large bacterial populations and have respiratory rates faster than the bulk sediment. He also concluded that smaller rapidly respiring particles are more likely to experience O_2 depletion at their centres than larger slower respiring niches. Ambient porosity of 0.9 with a microniche value of 0.7 (ml cm^{-3}) was used. This gave an effective microniche diffusion coefficient within the niches of 61% of the porewater value. Jahnke (1985) stated that when modelling the effects of microniches on a whole system, the volume-integrated OM degradation rate (the overall rate accounting for processes at microniches as well as in the bulk sediment) must remain constant. This therefore exerts a control on the number of microniches and/or the OM degradation rates at the niches. In practice this means that if the degradation rate of microniches increases, then fewer microniches must exist per unit volume. Jahnke (1985) showed that the maximum respiratory rate (per unit volume of sediment) of one millimetre diameter microniches is inversely correlated to the number of particles, with a factor of ten decrease in the number of particles yielding a ten times increase in maximum niche respiratory rate.

There are two key limitations to both the Jorgensen (1977) and Jahnke (1985) modelling. Firstly, by not considering electron acceptors other than O_2 and nitrate, the

likelihood that localized oxygen penetration will be decreased by oxidation of localised elevated concentrations of reduced components (e.g. NH_4^+, $\sum S(-II)$, Fe^{2+}, Mn^{2+}) is excluded. Secondly, by assuming homogeneous conditions around the microniches, the complex 3D distribution of solutes that occurs within the sediment is not considered. As both models considered niches within the oxic zone, it is likely that strong gradients will occur within the niches as well as within the surrounding sediment. This effect will be even more exacerbated where the ambient and niche porosities are different.

Brandes and Devol (1995) modelled microniches within a two-dimensional gridded domain (one square centimetre), to explain observations of simultaneous O_2 and NO_3^- respiration obtained from whole core squeezing experiments. They suggest that, in addition to organic carbon microniches, mixing of reduced inorganic material into the oxic zone may also be important in creating micro-zones of oxidizable material that consumes oxygen. The gridded area contained a distribution of <20, 100 µm diameter microniches, with high respiration rates. Their relative positions were adjusted (by eye) to obtain a best fit to the experimental data. With the assumed carbon concentration and O_2 respiration rates, the estimated particle lifetime was 15 days. Given the niche lifetimes measured/estimated from other studies (e.g. 2.5 days, Alldredge and Cohen, 1987; <5 days, Zhu et al, 2006), the particle respiration rates may be underestimated. However, Brandes and Devol (1995) did suggest that if the system were modelled in 3D, for the same result it would require fewer particles with higher reaction rates and hence shorter lifetimes.

2   Aims and scope of the thesis

The aims of this thesis were fourfold:

1. To critically review the literature of previous studies of microniches using high resolution probes and modelling approaches.

2. To develop a binding phase for the DGT technique, to enable analysis of oxyanions in sediment at high resolution, and to apply this technique to investigate processes occurring at a sulphidic microniche within a freshwater sediment.

3. To investigate the relationship between trace metal (cobalt) and iron and manganese in a marine sediment using DGT.

4. To apply a three-dimensional diagenetic model to investigate conceptually the geochemical behaviour of microniches under different conditions and to interpret these observations in terms of data from the literature and known trace element geochemistry.

3   Descriptions of individual papers

3.1   Paper I

Paper I is a critical review of the literature on the experimental evidence available on the existence of micro-heterogeneity in sediments, in essence forming an extended introduction to the thesis. The review covers the historical development of studies of micro-heterogeneity, current technologies used to elucidate their presence and suggests how future studies may be better focussed. Whilst the review covers the study of burrow microenvironments as well as microniches, each section is concluded with a description of the evidence for the existence of microniches. The rationale for the study of microniches is covered in this paper and is therefore excluded from the introduction.

3.2   Paper II

Paper II describes the methods for preparation, deployment and analysis for a combined silver iodide-ferrihydrite binding phase (within a hydrogel) for the diffusive gradients in thin-films (DGT) technique. The gel allows simultaneous analysis of phosphorus, sulphide, vanadium and arsenic. Results from laser ablation of the gel obtained at a sulphidic microniche in a freshwater sediment are discussed in terms of the potential geochemistry.

3.3   Paper III

Paper III presents observations revealed from multiple DGT deployments in a marine (Fleetwood Marina, UK) sediment. Aged sediments and fresh intact incubated cores yielded different relationships between Fe/Mn and cobalt. This study is not related directly to microniches. However, both understanding resupply to the DGT device and determining the relationships between trace metals and authigenic oxides are potentially important to the study of microniche geochemistry.

3.4   Paper IV

Paper IV presents the formulation and use of a diagenetic model designed specifically to investigate geochemistry at, or induced by, microniches. The complete framework of the model is described. The model is then applied to a hypothetical scenario, where microniches exist a few millimetres below the sediment water interface. The oxygen, nitrate and sulphide concentrations are discussed in terms of how they are affected by the niche.

3.5   Paper V

Paper V extends the microniche modelling undertaken in Paper IV by considering the effect of organic matter degradation rates and porosity on the life-span of a niche. Sulphide evolution in a niche below the nitrate penetration depth is discussed in terms of iron-sulphide formation. The potential trace metal diagenesis at microniches is discussed with reference to observations reported in the literature.

I.   Stockdale, A., Davison, W., Zhang, H., 2009. Micro-scale biogeochemical heterogeneity in sediments: A review of available techniques and observed evidence. Earth-Science Reviews, 92, 81-97. http://dx.doi.org/10.1016/j.earscirev.2008.11.003

II.   Stockdale, A., Davison, W., Zhang, H., 2008. High-resolution two-dimensional quantitative analysis of phosphorus, vanadium and arsenic, and qualitative analysis of sulfide, in a freshwater sediment. Environmental Chemistry, 5, 143-149. http://dx.doi.org/10.1071/EN07096

III.   Stockdale, A., Davison, W., Zhang, H., Hamilton-Taylor, J., 2010. The association of cobalt with iron and manganese (oxyhydr)oxides in marine sediment. Aquatic Geochemistry. http://dx.doi.org/10.1007/s10498-010-9092-1

IV.   Sochaczewski, Ł., Stockdale, A., Davison, W., Tych, W., Zhang, H., 2008. A three-dimensional reactive transport model for sediments, incorporating microniches. Environmental Chemistry, 5, 218-225. http://dx.doi.org/10.1071/EN08006

V.   Stockdale, A., Davison, W., Zhang, H., 2010. Sulfide evolution from faecal pellets and other microniches within sub oxic surface sediment. Geochimica et Cosmochimica Acta. http://dx.doi.org/10.1016/j.gca.2010.02.005

Sulphide evolution from faecal pellets and other microniches within sub oxic surface sediment: The effects on the geochemistry of iron and trace elements

Anthony Stockdale, William Davison*, Hao Zhang

Department of Environmental Science, Lancaster Environment Centre (LEC), Lancaster University,
Lancaster LA1 4YQ, United Kingdom

*Corresponding author. Fax +44-1524-93985.
E-mail addresses: a.stockdale@lancaster.ac.uk (A. Stockdale), w.davison@lancaster.ac.uk (W. Davison),
h.zhang@lancaster.ac.uk (H. Zhang).
Fax +44-1524-93985.

Abstract

Direct introduction of particles within sediments, such as faecal pellets, as well as biotic translocation of surface deposited material to greater depths, can lead to heterogeneously distributed particles of localized highly reducible organic matter (microniches) being present at depth. Where O_2, NO_3^-, and Fe/Mn oxyhydroxides become depleted within microniches or where they exist in zones of sulphate reduction, significant localized peaks in sulphide concentration can occur. These discrete zones of sulphide can cause specific localized diagenesis, affecting iron as well as trace elements. We have used a reaction-transport model developed specifically for investigating spherical microniches, and incorporating 3D diffusion, to investigate how the rate of organic matter (OM) degradation and the particle porosity affect sulphide and iron concentrations and the saturation index (SI) at such niches. For all of the modelled scenarios the SI for iron sulphide is positive, indicating conditions for FeS precipitation in all niches. Those simulations within the microniche lifetime (the time taken for the niche OM to reach 35% of its initial value, $t_{35\%}$) range of 2.5 to 5 days gave comparable concentration ratios of sulphide to iron in solution within the niche to experimentally observed values. Decreasing porosity, lower $t_{35\%}$ values and increasing OM degradation rates all tend to increase the likelihood that peak FeS precipitation will preferentially occur at the edges of the niche rather than uniformly throughout its volume. For trace elements forming sulphide precipitates, the saturation conditions evolve quickly (minutes) after the particle is introduced. Faecal pellets and other microniches may be important zones of FeS and trace metal sulphide formation in sediments and provide mechanism for metal removal within the oxic and suboxic zones, where formation of sulphides would not be predicted by analysis of the bulk sediment. These processes have implications for understanding the diagenesis of Fe and trace metals, and for our knowledge of the mechanisms for organic material preservation in the fossil record.

1. INTRODUCTION

In stable sediment where oxygen is present at the sediment water interface, bioturbation influences the sediment structure. Due to burrow formation, irrigation, feeding and associated processes, this influence often extends some way into the zone of the sediment usually considered anoxic. These processes create distributions of localized geochemical features as a result of, active burrows (with surface connection), inactive and infilled burrows, and faecal pellets, as well as translocation of surface deposited material, such as marine snow, to greater depths. Here we consider that microniches are formed when discrete particles of reactive organic matter are introduced at depth in the sediment. These microniches can be attributed to decaying organisms (observed using a pH optode; Zhu et al, 2006), algal aggregates (added to

sediment to study sulphidic microniches; Widerlund and Davison, 2007) and faecal pellets (photographed after resin embedding and thin sectioning of an intact core; Watling, 1988). Within vegetated sediments such as mangroves, root systems can also generate microniches (e.g. Alongi et al, 2004). The diameter of these microniches can in principle vary from a few microns up to the centimetre scale. However, using high-resolution probes their diameter has generally been observed in the range of 400 μm to ~1 cm (Stockdale et al, 2008; and references therein).

Where microniches become depleted in O_2, NO_3^-, and Fe/Mn oxyhydroxides or where they exist in zones of sulphate reduction, significant localized peaks in sulphide concentration can occur. Elevated sulphide within these microniches results in conditions where the formation of metal sulphides is optimised. Within the upper iron-dominated zone of marine sediments, localized pyrite is commonly associated with microniches (Raiswell, 1993). To

date, scant consideration has been given to how localized concentrations and microscale processes will affect, temporally and spatially, the formation of metal sulphides and favour particular reaction mechanisms in particles such as faecal pellets. It is difficult to do this by measurement as techniques that allow measurement on an appropriate scale are just being developed now. The stochastic nature of the processes means that it is likely to be many years before a true representative and comprehensive data set is available. In the absence of experimental data, modelling can be used to advance understanding in this field. Subsequent sections of the introduction examine previous modelling of microniches, evaluate the trace element/sulphide behaviour and niche geochemistry that is relevant to this work, and finally describe the aim and rationale of this work.

1.1. Trace Element/Sulphide Geochemistry

Several studies have compared reactive and pyrite bound fractions of trace metals, based on whether their proportion extracted with nitric acid (the final stage of a sequential leaching process) is more, less or similar to that of iron (Huerta-Diaz and Morse, 1990, 1992; Otero and Macias, 2003). The two parameters, degree of pyritization (DOP; Berner, 1970) and degree of trace metal pyritization (DTMP), are measures of the extent to which reactive iron is transformed into pyrite (DOP) and reactive trace metal is incorporated into pyrite (DTMP). These concepts were introduced to try to account for the quantities of metal present outside of a sulphide phase (influenced by e.g., adsorbing surfaces) where sulphide precipitation is favourable (Huerta-Diaz and Morse, 1992). Equations 1 and 2 show how these data are calculated.

$$DOP(\%) = \frac{\text{Pyrite-Fe}}{\text{Pyrite-Fe} + \text{Reactive-Fe}} \times 100 \qquad (1)$$

$$DTMP(\%) = \frac{\text{Pyrite-TM}}{\text{Pyrite-TM} + \text{Reactive-TM}} \times 100 \qquad (2)$$

Trace elements can be placed into three distinct groups based on the observed DTMP versus DOP (Figure 1). Morse and Luther (1999) assessed the early diagenetic geochemical processes that may affect the incorporation of trace elements into pyrite. Table 1 shows the phytoplankton element- carbon ratios reported in the literature and the early diagenetic processes that, according to Morse and Luther (1999), may affect the DTMP. These explanations for the observed behaviour indicate possible mechanisms of initial trace element reactions with sulphide and FeS, and the group within which an element falls may give an indication of how they behave within highly sulphidic microniches. For example, elements that exist as oxyanions will undergo reduction to yield species that are either more susceptible to scavenging as sulphides (e.g. Mo or As), or resistant to reaction with sulphides (e.g. Cr). Where ionic trace element sulphides are more susceptible to scavenging by FeS (e.g. MoS_4^{2-}; Helz et al, 2004) they may be more likely to be incorporated into pyrite. Other
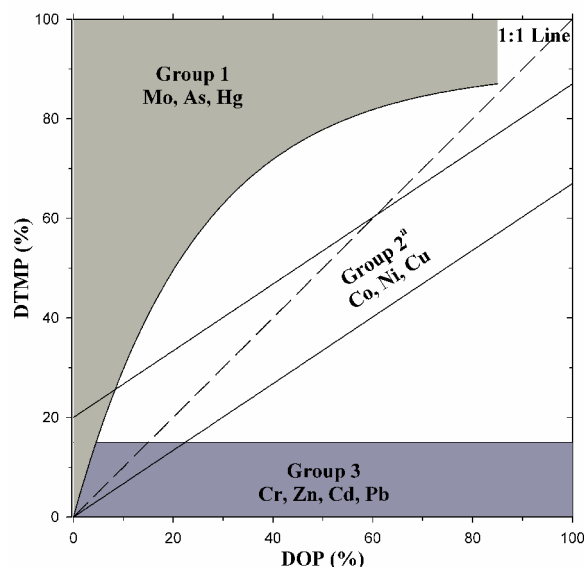
Figure 1. Degree of trace metal pyritization (DTMP) vs. degree of pyritization (DOP). Based on data in Huerta-Diaz and Morse, (1992) and Otero and Macias, (2003). A similar figure was presented in Burdige (2006). [a]Cu is included in Group 2 for simplicity, however the data tend to follow the 1:1 line more closely than represented here.

metals (Zn, Cd, Pb) react at a faster rate with sulphide (relative to Fe) and may form metal sulphides independent of pyrite.

1.2. Geochemistry of Microniches

Localized elevated sulphide coupled with trace element supply, resulting for example, from the oxidation of organic matter or diffusion of trace elements into a microniche from the surrounding sediment, may result in environments where trace element sulphide formation is significantly higher than values observed from bulk measurements. For example measurements such as core slicing, where mixing of redox regimes may result in loss of observable sulphides via oxidation. If such sulphides are not subsequently re-oxidized, microniches may account for a significant proportion of trace element accumulation. Widerlund and Davison (2007) observed numerous 2D images of sulphidic microniches in a freshwater sediment using diffusive gradients in thin films (DGT). They calculated that the proportion of the probe area occupied by sulphidic microniches was approximately one to four percent of the total probe area, indicating that in some sedimentary environments, microniches (and their associated elevated degradation rates) are significant in terms of the fraction of organic matter reduced. High resolution DGT has also demonstrated that cationic trace metals can be released at sulphidic microniches (Motelica-Heino et al, 2003). Conversely, depletion of phosphate and oxyanions of trace elements at a microniche has been observed at a sulphidic niche using similar techniques (Stockdale et al, 2008a).

Table 1. Pyritization group, phytoplankton element/carbon (E:C) ratios, and geochemical reasons for pyritization behaviour, for a range of elements.

DTMP: DOP group	Element	E:C (mol mol^{-1} (× 10^{-6}))	Ref.	Reasons attributed to trace element pyritization behaviour (Morse and Luther, 1999)
0	Fe	49	(1)	
		61	(2)	
1	As[a,b,c]	2.7	(3)	Oxyanions, first reduced by sulphide, may subsequently react with sulphides resulting in incorporation into pyrite.
	Mo	0.24	(2)	
	Hg[b]	0.0065	(4)	Chloride complexation retards reaction with sulphide, displacement reaction with FeS yields HgS. This can only be dissolved in the pyrite fraction, making distinction between HgS and pyrite phases impossible.
2	Co	1.5	(2)	Slower water exchange kinetics than Fe^{2+}; FeS phase precipitates and metals are subsequently incorporated into pyrite.
	Ni	2.7	(1)	
	Cu	2.7	(1)	Reduced by sulphide; forms a variety of sulphides both with and without Fe.
		3.1	(2)	
3	Cr[b,c]	4.1	(5)	Oxyanion reduced to a form that is kinetically inert to reaction with sulphide.
	Zn	12.5	(1)	
		6.5	(2)	Faster water exchange kinetics than Fe^{2+}, (Zn, Cd, Pb)S phases precipitate prior to FeS, resulting in low fractions of pyritized metal.
	Cd	2.5	(1)	
		1.7	(2)	
	Pb[b,c,d]	1.1	(6)	

(1) Bruland et al (1991) citing Martin and Knauer (1973) and Martin et al (1976), averaged values. (2) Ho et al, 2003. (3) Michel et al (1998). (4) Bargagli et al (1998). (5) Ebihara et al (2006). (6) Bu-Olayan et al (2001). [a]Estimated value. [b]Converted from µg/g(dw) by assuming 35g (dw) of phytoplankton contains 12g (one mole) of C. [c]Potential contamination sources near study sites. [d]Value from the site with the lowest Pb value for seawater.

1.3. Modelling of Microniches

Jørgensen (1977) pioneered modelling of microniches, investigating the conditions required for a niche to become anoxic within oxic sediment. This work and subsequent work by Jahnke (1985) considered scenarios where concentrations of possible reactants in the porewater surrounding the niche were homogeneous. Brandes and Devol (1995) extended the concepts to include multiple niches and associated gradients for O_2 and NO_3^-, in two-dimensions. Raiswell et al (1993) recognised that understanding localized iron-sulphide precipitation may be of value in paleoenvironmental studies and formulated a basic, 3D, three-component model (dissolved Fe and sulphide and a pyrite precipitate) relating diffusion and precipitation at the edge of spherical microniches of diameters 50 µm or more. The model assumed that sulphide diffuses away from the niche and reacts with dissolved iron to form precipitates. The modelling assumed that there is a constant (infinite) fixed pool for each of the solute components. The sulphide pool associated with the niche and the iron pool from the bulk surrounding sediment. Between these pools, at the edge of the niche, there is a reaction zone where diffusion and precipitation occur. The modelling showed that a greater niche diameter or higher sulphate reduction rate, required increasingly high dissolved iron concentrations to constrain pyrite precipitation to the niche edge (Raiswell et al, 1993). If the niche size is increased and the Fe is kept constant this would allow a greater proportion of the niche sulphide to diffuse further from the niche

before reacting with iron, leading to a lack of preservation of a pyrite imprint at the niche.

Multi component modelling in 3D has revealed further complexity in microniche geochemistry. Sochaczewski et al (2008), showed that within a single microniche near the sediment surface, there can be up to three discrete zones characterised by the dominance of different oxidants (O_2, NO_3^- and SO_4^-). It was assumed that there was no Fe or Mn oxides in the niche, which represents a parcel of organic matter. Sulphide is produced because O_2 and NO_3^- are readily consumed in the small volume of the niche.

1.4. Aims and Rationale of this Work

In the absence of appropriate experimental techniques, modelling can be used to advance understanding of processes occurring at localized highly labile particles such as faecal pellets or algal aggregates. 3D modelling gives a truer result as it allows lateral diffusion around niches that is not accounted for in 1D simulations. Here we modelled, in 3D, an idealised spherical particle with different values applied to the variables porosity and organic matter degradation rate. The modelling was undertaken without use of any fitting parameters so that any correlations to experimentally observed data are on an a priori basis. There were two main aims of this study. Firstly, to examine how a range of porosities and OM degradation rates affect sulphide and iron concentrations within microniches and to discuss how the results are related to observations and hypotheses from previous studies. Secondly, to assess how the modelling results are applicable to trace element diagenesis.

2. MODELLING FRAMEWORK

2.1. Model Description

The sediment model 3D TREAD is a fully three-dimensional diagenetic model specifically designed to investigate diagenetic processes occurring at spherical microniches. A brief description of the model is given here, for a more comprehensive account see Sochaczewski et al (2008).

The complexity of any simulation in 3D TREAD is dependent upon the number of modelled components and reactions specified by the user. Rather than providing a rigid framework where components and reactions are fixed, the model lets users specify all required parameters. For each individual component the following conditions can be set: boundary conditions for the top and bottom of the domain; diffusion coefficients; microniche radius, coordinates and concentration; initial profiles (for t = 0 s). Reactions and their rates are then specified for the listed components. Reactions can be specified as primary (i.e. organic matter decomposition) or secondary, with primary reactions requiring specification of a priority component (the OM oxidant) and a concentration threshold, below which the reaction with the next priority can begin to proceed. Secondary reactions can be specified as first order for each reactant (overall order based on the number of reactants) or first order for a single component only (overall order of one).

The domain parameters required include: domain size (x, y and z lengths), resolution (this controls the density of the 3D mesh), total simulation run time, the time step between each calculation, and the time step between each data save (this allows the output file size to be constrained and reduces output processing times). The porosity profile (and distinct values for each microniche) together with the equation for tortuosity (and associated variables) complete the parameterization of the model. As the model inputs are entered via a graphical user interface, parameters can be altered easily, allowing a range of scenarios to be tested.

2.2. Setup of Model Simulations

The reactions applied to the modelling are shown in Tables 2 and 3 (primary and secondary reactions respectively). Full model parameters (required inputs as described in section 2.1.) are provided in the supporting information as Table S1.
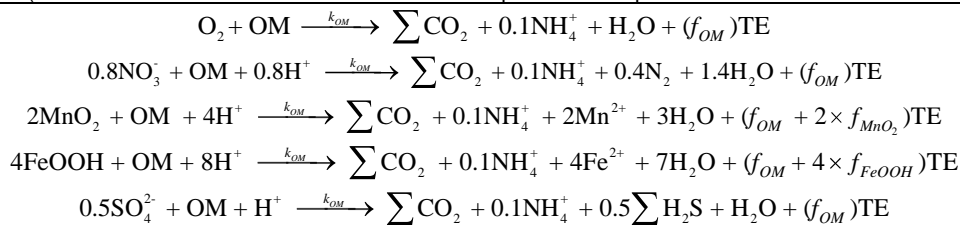
Table 3. Secondary reactions included in the modelled simulations. H_2O, H^+ and S^0 are include in the reactions for balancing but are excluded from the model simulations. (f is the fraction of trace metal associated with the particular component and TE is the trace element).

$$NH_4^+ + 2O_2 \xrightarrow{k_6} NO_3^- + H_2O + 2H^+$$

$$2Mn^{2+} + O_2 + 2H_2O \xrightarrow{k_7} 2MnO_2 + 4H^+$$

$$4Fe^{2+} + O_2 + 6H_2O \xrightarrow{k_8} 4FeOOH + 8H^+$$

$$2Fe^{2+} + MnO_2 + 2H_2O \xrightarrow{k_9} 2FeOOH + 2H^+ + Mn^{2+}$$

$$H_2S + 2FeOOH + 4H^+ \xrightarrow{k_{10}} S^0 + 2Fe^{2+} + 4H_2O + (2 \times f_{FeOOH})TE$$

$$H_2S + MnO_2 + 2H^+ \xrightarrow{k_{11}} S^0 + Mn^{2+} + 2H_2O + (f_{MnO_2})TE$$

$$H_2S + Fe^{2+} \xrightarrow{k_{12}} FeS + 2H^+$$

$$H_2S + 2O_2 \xrightarrow{k_{13}} SO_4^{2-} + 2H^+$$

$$FeS + 2O_2 \xrightarrow{k_{14}} Fe^{2+} + SO_4^{2-}$$

The environmental framework (i.e. the sediment chemistry and properties) is based on a comprehensive data set for a marine sediment by Fossing et al (2002; 2004). The modelling and associated parameters in this study are partly based upon previous studies (e.g. Froelich et al, 1979; Van Cappellen and Wang, 1996; Wang and Van Cappellen, 1996; Rysgaard et al, 1998). These data include all of the required inputs with the exception of the microniche specification. As we model a smaller domain, boundary conditions are derived from the 1D sediment profiles presented by Fossing et al (2002; 2004).

Sulphide removal mechanisms were via diffusion and reaction with Fe^{2+} (discussed below). The niche size (diameter) was set at three mm (metal release was measured at a similar sized sulphidic niche in a freshwater sediment by Motelica-Heino et al, 2003). Porosity outside the niche was set as 0.83, consistent with the data compilation used for the bulk values. Microniche porosity was varied to examine its effect. The range considered was from high porosity (φ = 0.97, 0.9) to niches denser (φ = 0.8, 0.7) than the ambient value. Niches are assumed to have negligible iron or manganese oxides available for OM oxidation. Where the niche surface contacts the bulk sediment these oxidants are assumed to be available. The limited consequences of the presence of authigenic oxides within microniches is briefly discussed in section 3.4.2.1.

Table 2. Primary (organic matter) reactions included in the modelled simulations. H_2O, H^+ and $\sum CO_2$ are include in the reactions for balancing but are excluded from the model simulations. The full equations including f and TE are used in the calculations for Tables 4 and 5 (f is the fraction of trace metal associated with the particular component and TE is the trace element).

$$O_2 + OM \xrightarrow{k_{OM}} \sum CO_2 + 0.1NH_4^+ + H_2O + (f_{OM})TE$$

$$0.8NO_3^- + OM + 0.8H^+ \xrightarrow{k_{OM}} \sum CO_2 + 0.1NH_4^+ + 0.4N_2 + 1.4H_2O + (f_{OM})TE$$

$$2MnO_2 + OM + 4H^+ \xrightarrow{k_{OM}} \sum CO_2 + 0.1NH_4^+ + 2Mn^{2+} + 3H_2O + (f_{OM} + 2 \times f_{MnO_2})TE$$

$$4FeOOH + OM + 8H^+ \xrightarrow{k_{OM}} \sum CO_2 + 0.1NH_4^+ + 4Fe^{2+} + 7H_2O + (f_{OM} + 4 \times f_{FeOOH})TE$$

$$0.5SO_4^{2-} + OM + H^+ \xrightarrow{k_{OM}} \sum CO_2 + 0.1NH_4^+ + 0.5\sum H_2S + H_2O + (f_{OM})TE$$

2.3. Treatment of Iron-Sulphide Reactions

Iron sulphide precipitation/dissolution reactions are often modelled assuming reversible reactions, typically expressed as separate reactions for formation and dissolution. Whether or not the saturation conditions are met controls which of the two reactions can proceed (see, van Cappellen et al, 1993; Boudreau, 1996; Wang and van Cappellen, 1996 for details of this approach). This relationship is widely used in diagenetic models (e.g. Wijsman et al, 2002; Morse and Eldridge, 2007). However, in other modelling cases (e.g. Berg et al, 2002; Fossing et al, 2004) a simple unidirectional formation reaction has been applied (Eq. 3).

$$Fe^{2+} + \sum S(\text{-II}) \xrightarrow{k_{FeS}} FeS \qquad (3)$$
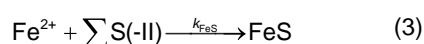
A significant advantage of using this approach is that the complexities of modelling pH changes within the model can be avoided. Furthermore, for our modelling this approach is appropriate, as saturation conditions are likely to apply throughout the small domain modelled. Thus the reverse process is negligible and can effectively be excluded.

3. RESULTS AND DISCUSSION

This section reports the results of the modelling and discusses them in terms of:

- trends in iron, sulphide and the related saturation index (SI) with changing porosity, OM degradation rate and niche lifespan.

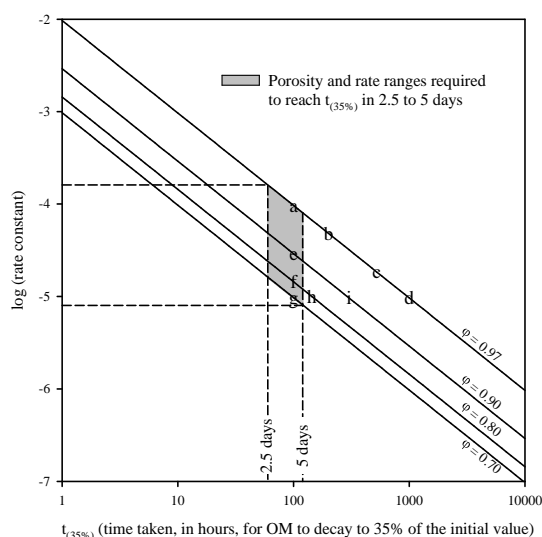- relating data from these trends to experimental observations

Figure 2. Relationship between the rate constant for the decomposition of organic matter (OM), porosity of the microniche, and the time taken (in hours) for the OM concentration to decay to 35% of the initial value. Letters represent individual data points used in model runs described in the text.

- assessing the optimum conditions for the formation of FeS crusts at microniches
- relating the modelled data to known behaviour of trace elements in terms of, trace element sources, reaction pathways, and solubility of trace element sulphides.

3.1. Description of Modelled Scenarios

Microniches with various properties were modelled. The effects of porosity and reaction rate of organic matter on the lifespan of a niche are shown to give a general overview, with specific examples considered in more detail to examine the generation of sulphide (and associated iron) profiles. The simulation conditions were devised to consider localized sulphide concentrations and the associated lifespan of the niches, while making comparisons with reported reaction rates and experimental observations of niche life-span. Modelling different porosities allow the results to be interpreted for a range of particle types, from high porosity niches such as algal aggregates to lower porosity particles such as faecal pellets.

3.2. Iron and Sulphide at Microniches

3.2.1. Trends Related to Porosity and Rate
Typically observed values for the rate of decomposition of OM, porosity and microniche size were used in the simulations, to ensure that the outputs can be related to realistic environmental scenarios. Figure 2 shows the relationship between reaction rate and microniche lifetime for niches with a range of porosities. Lifetime is operationally defined as the time taken for a niche to be degraded to 35% of the starting value ($t_{35\%}$). The lettered data points in Figure 2 represent three groups of data where one of the parameters is constant. Group A (a, b, c, d) has constant porosity, with the decreasing rate constant resulting in an increase in $t_{35\%}$ across the series. Group B (a, e, f, g) was obtained by setting a series of decreasing porosity and adjusting rate constants to give equal values for $t_{35\%}$ (100 hours). For Group C (g, h, i, d) the rate constant was maintained and $t_{35\%}$ calculated for the range of porosities. Fossing et al (2002; 2004), in modelling a marine sediment in 1D, used a multi-G approach to organic matter degradation (e.g. Westrich and Berner, 1984). They used a ratio for the rate constants of degradation of the fast and slowly degrading pools of OM of 800 ($k_{om\text{-}f} : k_{om\text{-}s}$). This $k_{om\text{-}f}$ rate constant was applied to the scenarios modelled in Group C. Within Group A, ratios of 800, 1600, 4000 and 8000 were used to generate outputs for d, c, b and a respectively. The $t_{35\%}$ values for Group B lay within the range of microniche lifetimes observed by Alldredge and Cohen (1987) and Zhu et al (2006).

Figure 3 shows, for each of the lettered groups, the sulphide and Fe^{2+} concentrations at the centre of the modelled microniches, and the saturation index (SI), which is related to the solubility
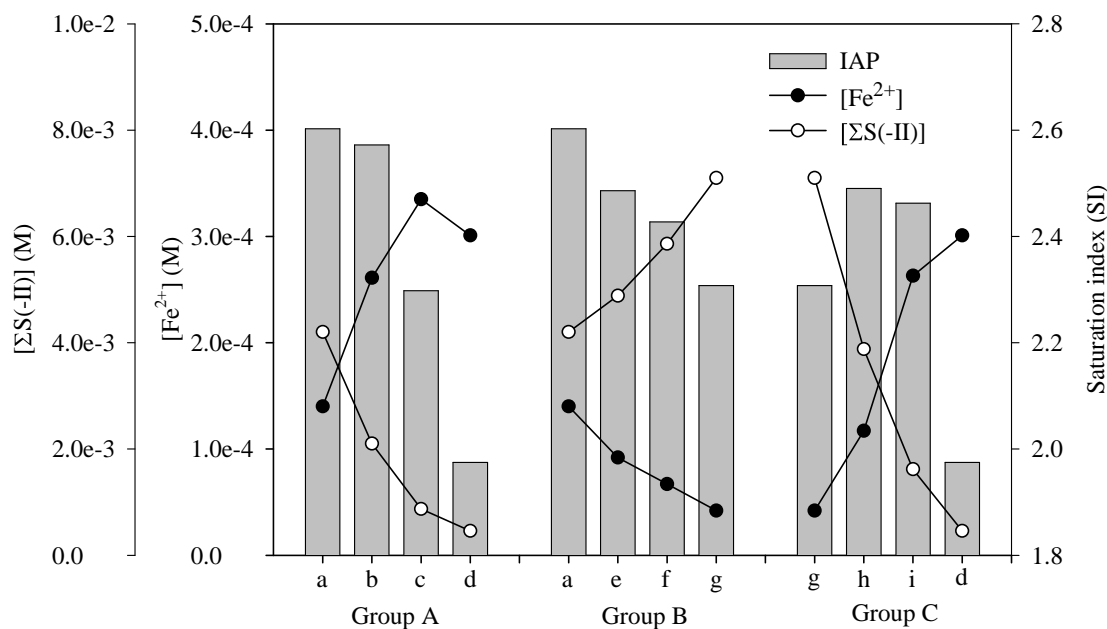
Figure 3. Predicted concentrations of sulphide and iron and the related saturation index (SI) after 2.3 hours of the simulations at the centre of a microniche. The letters represent the data points in Figure 2, where each group of letters has one variable set as a constant. Group A has constant porosity, Group B has conditions where $t_{35\%}$ is constant, Group C has a constant OM degradation rate. Note that the axis for the SI values does not start at zero.

product of FeS (K_{SP}) and the ion activity products (IAP; Eqs. 4 and 5).

$$IAP = \{Fe^{2+}\}\{HS^-\}/\{H^+\} \qquad (4)$$

$$SI = \log(IAP/K_{SP}) \qquad (5)$$

IAP was calculated assuming a pH of 7 (consistent with marine porewater values that are typically lower than the overlying water (e.g. Ben-Yaakov, 1973; Zhu et al, 2006) and ionic strength of 0.7 M, with activity coefficients of, γFe^{2+} = 0.255, γHS^- = 0.410, γH^+ = 0.958, (values for Fe^{2+} and H^+ were calculated using the Pitzer equation and associated variables as reported in Millero and Schreiber, 1982; bisulphide value is that reported in Davison, 1980).

Decreasing the rate constant and maintaining a fixed porosity (Group A) results in decreasing peak sulphide values, due to lower generation of sulphide fluxes within the niche. The Fe(II) concentration at the centre of the niche is determined by several opposing factors. As sulphide produced in the niche diffuses out, it reduces FeOOH in the surrounding sediment and the resulting Fe(II) diffuses in. Fe(II) is also supplied to the system as FeOOH is used as an electron acceptor at the niche edge. For scenarios with shorter life-spans, the FeOOH is depleted more rapidly, affecting the potential Fe(II) supply from this source. However, Fe(II) is also continuously removed at all locations by reaction with HS^- to form FeS. The peaked distribution for Fe can be ascribed to changes in the relative dominance of these three processes. The SI is strongly dependent on sulphide in this case.

Where OM degradation rate constants are adjusted for different porosity microniches to give equal lifetimes for all niches (Group B), diffusion and reaction with sulphide controls the peak values of Fe(II) and diffusion and the rate constant controls peak sulphide. As the porosity decreases, both diffusion and reaction rates lowered, decreasing both the inward iron flux and the outward flux of sulphide. In this marine system the sulphate removal rate is not high enough to cause this electron acceptor to become limited in any of the modelled scenarios. Iron tends to exert the main control on the SI within this group.

Where porosity (φ) is increased at a constant OM degradation rate constant (Group C) sulphide decreases due to a reduced flux caused by the lower physical amount of reactive OM within the niche (accounted for in the model calculation by a $(1-\varphi)$ function). Across this group the peak concentration of Fe(II) increases as diffusion is faster and removal by sulphide is lower. The highest values for the SI are observed at intermediate porosities. SI in this group is not controlled exclusively by one species. Within the lowest porosity niche it is constrained by limited diffusion of Fe(II) into the niche, while within the highest porosity niche it is constrained by lower sulphide concentrations caused by a reduced sulphide flux. These processes are represented visually in Figure 4, which shows 2D profiles of $\sum S(-II)$, Fe(II) and FeS after 24 hours for scenario g. Part d of this figure shows a schematic of how FeS may preferentially form at the edges of niche, which is shown by the modelled data in part c of the figure.
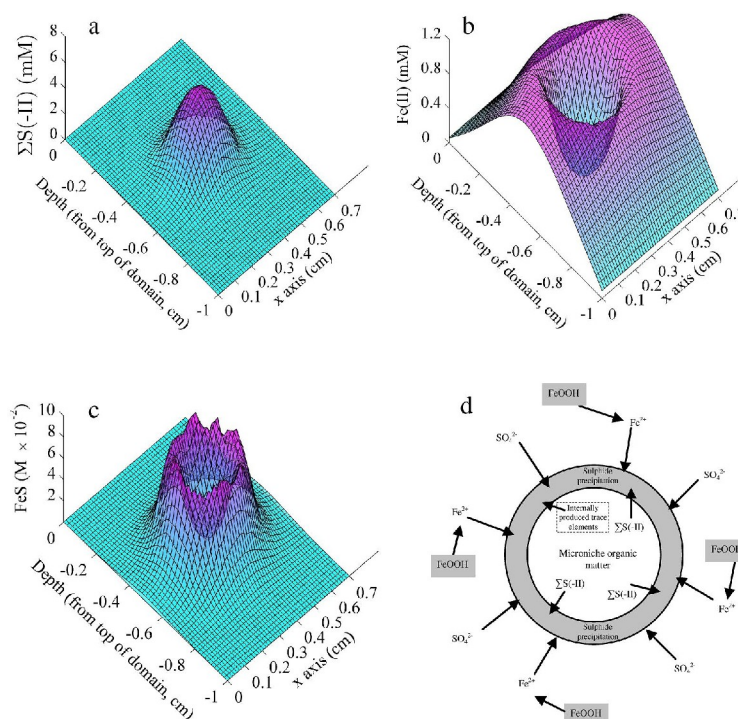
Figure 4. ∑S(-II) (a), Fe(II) (b) and FeS (c) concentration across the x axis of the modelled domain after 24 hours (y coordinate was the centre of the microniche). The microniche had a porosity of 0.7, an OM concentration of 5 M, and an OM degradation rate of 9.6×10^{-6} s^{-1} (scenario g in Figure 2). Part d, shows a schematic for the sulphide precipitation and solute fluxes into and from the microniche, modified from Berner (1980, p131).

### 3.2.2. Relating General Trends from the Modelled Data to Experimental Observations

Peak sulphide concentrations for the microniches are high when compared to bulk porewater values from electrode studies. For example, Sell and Morse (2006) reported a value of ~3 × 10^{-5} M for a marine sediment, approximately 2 cm below the oxygen penetration depth. If this value is representative of a background measurement, in the modelled microniche, peak concentrations are between ~15 and 240 times the background value. Using DGT to measure sulphide in a freshwater sediment, Motelica-Heino et al (2003), reported a sulphidic microniche with concentrations approximately 30 times the average background value. Sagemann et al (1999) set up laboratory experiments to determine conditions that may result in mineral formation at the soft tissue of benthic organisms (via precipitation of carbonates and phosphates as well as sulphides). They measured sulphide concentrations at the edge of a decomposing shrimp carcass of ~5.6 mM. This value fits into the range of values modelled here (0.46-7.1 mM).

The ratios of the total-sulphide to iron concentrations calculated from the data in Figure 3 fall in the range 1.6 to 169. When the lifetimes greater than 7 days are excluded (Figure 2, points b, c, d and i) are excluded, the lowest ratio is 30. For microniches within a freshwater lake sediment, sulphide concentrations have been observed to be over 40 times higher than those of Fe^{2+} (Motelica-

Heino et al, 2003). These agreements between measurement and modelling further supports the assertion that niche lifetimes of less than one week are the most representative of natural conditions.

3.3. Iron Sulphide at Microniches

The solubility of freshly formed iron sulphide in circumneutral sediment tends to be controlled by the solubility product related to the bisulphide concentration (Eq. 6).

$$FeS_{(s)} + H^+ \underset{\xrightarrow{\hspace{1cm}}}{\overset{K_{FeS}}{\rightleftharpoons}} Fe^{2+} + HS^- \qquad (6)$$
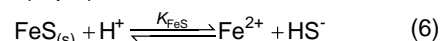
We calculated the distribution of sulphide species in simple sulphide solutions with a pH of 6, 7 and 8, an ionic strength of 0.7 and assuming [S^{2-}] is negligible (activity coefficients were, γH^+ = 0.96, γHS^- = 0.41 and γH_2S = 1.0). At pH 6, 7 and 8 approximately 19%, 70% and 96% respectively, of the total sulphide will be present as bisulphide. Within marine sediments pH has been observed over this range. Zhu et al (2006) using planar optodes, measured pH at a dead decaying organism (which can be considered a microniche) and reported pH at or below the lower detection limit of 5.9. Average pH between 1-6 cm below the sediment water interface, in the same sediment without the microniche but with burrowing activity, was ~6.8 with maxima of ~pH 8 and minima of pH ≤6.2. Using the SI data from Figure 3 (calculated at pH 7), the degree of saturation of FeS can be calculated. The lowest and highest values for SI are 1.97 and 2.6, equivalent to

a degree of saturation of 94 and 400 respectively. It is possible that levels of saturation will not reach these values due to the formation of other mineral phases.

Berner (1980) suggested that concretions of pyrite may be formed by heterogeneous reduction of sulphate at clots of organic matter. The sulphide reacts with Fe(II) diffusing towards the niche from the surrounding sediment to form iron sulphides that eventually transform to pyrite. The amount of FeS or pyrite formed is limited by the amount of decomposable organic matter in the niche and the resupply of Fe(II). Berner (1980) proposed that a crust of pyrite will form adjacent to the organic matter. When viewed in 2D as a cross section through the niche, the iron sulphide precipitate appears as a halo shape (Figure 4, part c). In modelling the lettered scenarios in Figure 2, we have determined the distribution of iron sulphide after 24 hours of each of the model runs. Figure 5 shows the vertical FeS profiles through the centre of each niche from these simulations and identifies the profile shape for each of the modelled scenarios. Simulations with $t_{35\%}$ values higher than seven days (b, c, d, and i) tend to have either undefined or poorly defined FeS peaks at the niche edges. Where the $t_{35\%}$ value lies within the 2.5-5 day range, peak FeS values are centred on the edges of the niche and peak values do not differ significantly (a, e, f and g). The greater the porosity of the niche, the lower the ratio of FeS at the edge of the niche compared to the centre of the niche. Scenario g shows the most significant halo effect and this is illustrated in 2D in Figure 4, part c.

The modelling has shown, a priori, that the concept described by Berner (1980) can be explained quantitatively by the microniche model, and that the niche life-times of 2.5-5 days give the best results in terms of the definition of the crustal nature of these iron sulphide deposits.

3.3.1. Relevance of 'Crustal' Deposition to Paleoenvironmental Studies

Although not the main focus of this study it is important to recognise the significance of the observed precipitation behaviour to the study of the preservation of microniches in the paleo record. Much work has focused on the processes involved in the preservation of soft-matter in the fossil record (e.g. Briggs et al, 1991; 1996; Raiswell et al, 1993; 2008). The conclusion that niche lifetimes of 2.5-5 days give better defined crustal deposition is supported by the work of Sagemann et al (1999). They concluded that: 1) Mineralization will be dominated by dysaerobic and anaerobic reactions, even in oxic sediments. 2) The most extensive mineral formation of soft tissues occurred under anoxic conditions. 3) Steep chemical gradients during the decay process lead to mineral formation. 4) Exceptional preservation of soft tissue is favoured by elevated microbial activity. 5) These critical controls that determine the balance between decay and mineral formation (points 1-4) must operate at an early stage following the death of an organism and mineral formation (leading ultimately to fossilisation) of soft tissue must be a rapid process
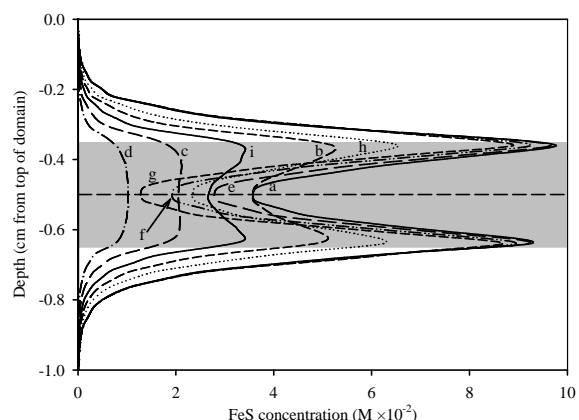
Figure 5. FeS concentrations after a 24 hour model simulation for each of the lettered scenarios in Figure 2. The shaded area represents the locations where the niche is present.

(days to weeks) as it would not occur at the normal bulk efficiency of OM degradation in marine sediments.

3.4. Relating Modelled Observations to Trace Element Diagenesis at Microniches

3.4.1. Modelling of Trace Element-Sulphide Reactions

Whilst modelling of general trace metal-sulphide interactions is limited, several studies have attempted to model zinc-sulphide reactions (Druschel et al, 2002; Choi et al, 2006; Canavan et al, 2007). These approaches (which are described and reviewed in more detail in the supporting information) tend to apply FeS formation rates to ZnS, which may not be accurate. More experimental evidence for reaction rates and determination of the significance of the different processes, is needed before such reactions can be modelled with any certainty. For this reason we considered that rather than attempting to model directly trace element behaviour at microniches, it was more appropriate to discuss the modelled observations for Fe and $\sum$S(-II) in terms of known trace element data such as sulphide solubility, trace element sources and known reaction pathways.

3.4.2. Trace Element Sources

The fractions of trace elements associated with phytoplankton organic matter (Table 1) are used to inform discussion of metal diagenesis at microniches. The majority of the data are taken from reported Redfield stoichiometries (Bruland et al, 1991; Ho et al, 2003). We recognise that there is likely to be large natural variability in different particles in the marine environment. Where microniches are formed from marine snow, the particles may undergo both loss and accumulation of some elements during settling (e.g. Fisher et al, 1991). Trace elements within faecal pellets from both pelagic and benthic organisms may be amended by digestion processes (e.g. Lee and Fisher, 1992 and references therein). Phytoplankton are the primary food source for many organisms and can be aggregated to form microniches, therefore, the trace

element ratio data are a suitable proxy for a range of niche types.

Table S2 is included in the supporting information to show the data used for trace metal concentrations (fractions) associated with authigenic oxides. Individual values for trace element fractions associated with both Fe and Mn authigenic oxides in Tessier et al (1996) are for freshwater sediments. Douglas and Adeney (2000) measured trace metals associated with Fe/Mn oxyhydroxides in marine sediments, but did not cite individual values for Fe and Mn oxides. Based on the high Fe:Mn ratio and assuming the values are just for authigenic Fe oxides, the concentrations in the mixed oxyhydroxide are ~2.5 times lower than the Tessier et al (1996) values. Therefore, the values used for authigenic Fe and Mn oxides are estimated as the Tessier et al (1996) values divided by 2.5. Using these data, Table 4 shows estimated trace element fluxes per mole of organic carbon (OC) per second for a niche with the same rate and porosity properties as scenario g. Each column of data in the table assumes that there is only one dominant electron acceptor degrading the OC. Where authigenic oxides are the dominant electron acceptor trace metal release at microniches may be significant. However, the extent to which these oxide concentrations are sustained within microniches is limited (discussed in the following section).

3.4.2.1. Microniches containing authigenic oxides. Degradation of OC involving authigenic oxides releases trace metal concentrations greatly in excess of the release attributed to organic matter alone (Table 4). It is unlikely that the supply of authigenic oxides will be sufficient to sustain element release from this source during a significant proportion of the niche lifetime, but it could be responsible for a pulse of metals from a localized source. To demonstrate this we modelled a scenario where the oxide concentrations at the nitrate penetration depth (0.67 cm; from the 1D profiles in Fossing et al, 2002; 2004) were applied to the niche, resulting in niches with oxide concentrations slightly elevated compared to the ambient sediment. The niche was assumed to have the same degradation rate regardless of the oxidant. Even for this situation favouring the presence of Fe/Mn oxides, they were consumed within the first 2-3 hrs of the model simulation. This effect was observed regardless of the whether limiting concentration thresholds, allowing successive electron acceptors, were set at the bulk values or 2% of this value. Additionally, loss of oxides by oxidation of the OM within the niche was much more significant than loss caused by chemical oxidation of sulphide (this work, unpublished results).

Elevated cationic metal concentrations observed at sulphidic microniches using DGT (for Co, Ni and Cu; Motelica-Heino, 2003) were attributed to concomitant release of sulphide and metal from the degrading niche. The observed elevated concentrations were 2-3 times the baseline concentrations observed outside the niche. It is possible that elevated trace metal may alternatively be attributed to an initial fast release

Table 4. Estimated maximum trace metal release (in mol per mol of organic carbon per second) resulting from different organic matter oxidation pathways. Assumes conditions the same as scenario g in Figure 2 (i.e. $\varphi = 0.7$, and rate = 9.6×10^{-6} s^{-1}). See Tables 1 and S2 for the element fractions data and Table 2 for the equations used. Elements are grouped according to their DTMP group (see Figure 1).

Element	Electron acceptor		
	O_2, NO_3^-, SO_4^{2-} (mol (mol OM)$^{-1}$ s^{-1} ($\times 10^{-12}$))	MnO_2 (mol (mol OM)$^{-1}$ s^{-1} ($\times 10^{-9}$))	FeOOH
As	7.78	-	-
Mo	0.69	-	-
Hg	0.019	-	-
Co	4.32	-	-
Ni	7.78	318	70.5
Cu	8.35	25.4	25.4
Cr	11.81	-	-
Zn	27.36	24.2	23.1
Cd	6.05	0.301	0.163
Pb	3.17	0.648	2.31

from microniche authigenic oxide sources rather than a gradual release from organic matter as it is oxidised by sulphate. The proportionally greater enrichment of observed Fe and Mn over their background values, than the trace metals (Motelica-Heino et al, 2003), gives further emphasis to this possible mechanism. If essential elements are taken up by the mediating bacteria, localized depletions in trace element concentrations may be expected. Localized low concentrations of phosphate and vanadium associated with sulphidic microniches were attributed to potential uptake by microniche bacteria (Stockdale et al, 2008a). Interpretation of DGT observed data should include an assessment of the potential effects induced by the device in its immediate vicinity (i.e. within 1-2 mm of its surface). For example, less sulphide will diffuse into the surrounding sediment from a microniche if it is adjacent to a DGT device, which removes some of the sulphide. Consequently there will be less sulphide available for chemical oxidation by authigenic oxides in the ambient sediment, which may result in lower trace metal release from these sources. Under unperturbed conditions, chemical reduction of ambient authigenic oxides by sulphide may promote a net diffusion of trace elements towards the niche, increasing their significance in terms of trace metal sulphide formation.

3.4.3. Trace Element Reaction Pathways

Studies of molybdenum sulphide reactions provide examples of how the concentration of sulphide may affect the initial processes that act as a precursor to pyritization, such as chemical reactions with sulphide and adsorption of sulphidic forms. Zheng et al (2000) found that a threshold sulphide concentration of ~10^{-7} M had to be exceeded before Mo co-precipitates with Fe-S. Direct Mo precipitation (as Mo-S or particle bound Mo) required a sulphide

Table 5. Trace metal sulphide solubility products[a] for the least crystalline sulphide of each metal. Metal released from a microniche over 60 seconds[b] and trace metal saturation thresholds[c].

Metal sulphide	K_{sp}	Activity coefficients[d] (γMe^{2+})	Metal release at microniche (M)	Saturation threshold (M)
FeS(am)	1.12×10^{-3}	0.255	-	7.34×10^{-7}
CoS(α)	3.98×10^{-8}	0.260	1.3×10^{-9}	2.56×10^{-11}
NiS(α)	3.16×10^{-6}	0.268	2.3×10^{-9}	1.97×10^{-9}
CuS	5.37×10^{-23}	0.220	2.5×10^{-9}	4.08×10^{-26}
ZnS(am)	9.55×10^{-10}	0.266	8.2×10^{-9}	7.06×10^{-13}
CdS(am)	1.00×10^{-13}	0.641	1.8×10^{-9}	2.61×10^{-17}
HgS	3.16×10^{-39}	0.250	5.7×10^{-12}	2.11×10^{-42}
PbS(galena)	5.62×10^{-13}	0.312	9.5×10^{-9}	3.01×10^{-16}

[a]Solubility products for the reaction $MS_{(s)} + H^+ \leftrightarrow M^{2+} + HS^-$ K_{sp} values from Huerta-Diaz et al (1998, and references therein), except HgS, from Di Toro et al (1992, and references therein). [b]Assuming niche has an OM concentration of 5 M and applying values for non-metal oxide electron acceptors from Table 4. [c]Trace metal saturation thresholds are the minimum metal concentrations required for saturation conditions to be met. These calculations assume a pH of 7, a peak total sulphide concentration of 2×10^{-3} M (met by all simulations except c, d and i; additional activity coefficients used were, $\gamma H^+ = 0.958$ and $\gamma HS^- = 0.410$). [d]Activity coefficients were calculated from the Pitzer equation and variables reported in Millero and Schreiber (1982), except Hg which is an assumed value.

concentration exceeding $\sim 10^{-4}$ M. A study by Erickson and Helz (2000) on Mo speciation in sulphidic waters (Black Sea) suggested that at a sulphide concentration of $\sim 1.1 \times 10^{-5}$ M, molybdate (MoO_4^{2-}) is converted to tetrathiomolybdate (MoS_4^{2-}) without yielding significant concentrations of intermediates. Tetrathiomolybdate has been shown to adsorb more strongly than molybdate to pyrite in anoxic sediments (Bostick et al, 2003). Helz et al (2004), suggested that potential diffusion of Mo into sulphidic microenvironments and subsequent fixation could be misinterpreted as fixation at low ambient sulphide concentration.

All of the scenarios we have modelled result in sulphide peaks (at the niche centre) greater than 10^{-3} M. This suggests that Mo within, or diffusing to, microniches will precipitate directly rather than co-precipitate with FeS. Analogous thio intermediates to Mo have been identified for arsenic (Wallschläger and Stadey, 2007) indicating that the sulphide reaction mechanisms may also be analogous. This is also suggested by the reported similarity in their DTMP versus DOP data (Figure 1). Microniches may therefore also have a similar impact on arsenic diagenesis. The summary of the metal sulphide reaction mechanisms suggested in Morse and Luther (1999) shown in Table 1, indicates that several different pathways exist for trace element reactions with sulphide. In addition to these mechanisms Di Toro et al (1990; 1992), have shown that Cd can undergo a displacement reaction with FeS to form a cadmium sulphide precipitate. They propose that similar reactions operate for other metals with lower sulphide solubility products than FeS (i.e. for Hg, Pb, Zn and Ni). At microniches, sulphide reactions of these trace elements as they diffuse into the niche from the ambient sediment may be more likely to be controlled by the displacement mechanism, as once established the FeS peak will be encountered before the sulphide peak in most of the modelled scenarios (as shown by the 2D images in Figure 4). Metal concentrations within the niche may be controlled by a balance between the relevant reactions and a combination of removal by direct sulphide

precipitation and the displacement mechanism, depending upon the niche lifetime and therefore the FeS concentration.

3.4.4. Trace Element Sulphide Solubility

Table 5 shows the solubility products and saturation thresholds of several trace metal sulphides for the reaction of the metal with bisulphide. The saturation thresholds represent the concentration of metal that needs to be exceeded for supersaturation conditions to exist at the centre of the niche (where the sulphide peak is observed). These values were calculated assuming a pH of 7 and a peak sulphide concentration of 2×10^{-3} M, which is met in all of the modelled scenarios except c, d and i (where peak total sulphide concentrations are 4.6×10^{-4}, 8.7×10^{-4} and 1.6×10^{-3} M respectively). The low solubility of many of these sulphides coupled with the very high peak sulphide concentrations, results in threshold concentrations of metals below 2×10^{-9} M for all sulphides except iron. When comparing these thresholds with the potential release of trace metals from OM (Table 5; assuming a OM concentration of 5 M and a 60 second time period), it is tempting to suggest that the release from organic matter within the microniche may be sufficient to buffer the element concentrations above the threshold values. However, this will depend on the reaction rates between trace elements and sulphide, the removal rate to other sinks (e.g. adsorption) and the extent to which trace elements in the OM are utilised by the bacteria facilitating the decomposition. Given the high sulphide concentration and the continuous release of trace elements, it is possible that there will be continuous trace metal sulphide formation throughout the lifetime of the niche. Where a niche exists in a zone of ambient authigenic oxide degradation, additional trace metal may be supplied to the niche. Trace element release from the authigenic oxides reduced during OM oxidation in the bulk sediment will be approximately a thousand times less than those values quoted for degradation at microniches in Table 4 (Based on the Multi-G rates from Fossing et

al, 2002). Despite this, the supply of some elements from this external source will still far exceed the microniche-OM supply due to the high concentrations associated with the oxides. This is particularly the case for Ni.

Sulphide evolution in particles above 1 mm in diameter within the oxygen and nitrate reduction zones has also been predicted (Sochaczewski et al, 2008). Faecal pellets and other microniche may be important zones of FeS and trace metal sulphide formation in sediments and provide mechanism for metal removal within the oxic and suboxic zones, where formation of sulphides would not be predicted by analysis of the bulk sediment.

3.5. Other Considerations

3.5.1. Explaining the Fe(II) Profiles

Exclusion from our model of typical parameters, such as those that account for bioirrigation and biodiffusivity, is appropriate given the nature of our modelling. It may be reasonable to expect that in a real system there will be small zones where these parameters have no or little effect, at least over time scales of a few days. In our simulations the concentration of Fe(II) can build up to levels much higher than if these parameters were included (Figure 4b). The presence of fixed boundaries at the top and bottom of the domain result in an imposed flux out of the domain. In a heterogeneous system with bioturbation, there are likely to be localized zones where solutes diffuse toward secondary interfaces, such as burrows. We accept that our modelled scenarios may be simplistic in the treatment of such behaviour. However, the small-scale modelling we have attempted is not open to the treatment of bioturbation and irrigation as averaged processes. In using diagenetic data from a combined experimental and modelling study we have excluded any fitting parameters for bioturbation processes in order to give results that reflect what may occur at and around microniches.

It has been suggested that for microniches greater than 100 μm diameter formed from rapidly metabolising soft tissue, the greater the production of sulphide (from either larger niches or higher sulphate reduction rates), the higher the concentrations of porewater iron required in order to confine FeS precipitation to the decay site (Raiswell, 1993; Raiswell et al, 1993; 2008). Thus the complexity of the effect of the iron concentration is governed not only by the bulk concentration, but also by the local concentration, the OM microniche radius, and the OM degradation rates for both the niche (affecting sulphide production) and the bulk sediment (affecting porewater Fe in sediment zones where iron (oxyhydr)oxides are the dominant electron acceptor). The effect of lower iron concentrations on pyrite precipitation at microniches has been investigated experimentally (Allen, 2002).

3.5.2. Influence of Microniche pH

For simplicity we have assumed a microniche pH of 7 for all calculations in this work. However, complex distributions of pH may occur at microniches, Zhu et al (2006) observed pH at a dead decaying organism of ≤5.9, where the ambient pH was ~6.6. Diffusion of protons away the niche results in a concentration gradient extending from the niche. As pH becomes lower IAP's are reduced by two contributing factors. Firstly, the pH term in the denominator of the equation, and secondly the equilibrium of sulphide species is shifted towards the H_2S species. The result will be to reduce the formation rate for sulphides at the centre of the niche. As the proton concentration gradient extends from the niche, this effect may enhance FeS formation at the niche edges and result in more contrast in the halo effect.

3.5.3. Potential Influence of Diffusive Barriers Around Microniches

In the modelling reported here we have assumed that solute transport into and from the niche is controlled exclusively by diffusion (accounting also for the changes to diffusion coefficients induced by porosity changes). Microniches in nature (including faecal pellets and decaying organisms) will have a range of diffusional barriers which will retard or prevent diffusion across the niche edge. Faecal pellets may possess peritrophic membranes, dead tube dwelling organisms may have a mucus membrane lining the burrow wall at is edge, soft parts of shelled organisms will only have limited exposure to the bulk sediment, and decaying organisms with hard-parts may have complex structures that affect diffusion (see also Stockdale et al, 2008). Where precipitates form surrounding a niche, it is possible that this will create a barrier to diffusion. How diffusive restrictions effect the formation of sulphide precipitates will largely depend upon the resupply of sulphate to the niche interior. In a scenario where diffusion is restricted yet sufficient to resupply sulphate, restriction in the efflux of sulphide will reduce the porewater Fe concentrations that is required for precipitation at the niche edge, consistent with the conclusions of Raiswell et al (1993) discussed in section 1.3.

4. CONCLUSIONS

We have modelled the behaviour of sulphide and iron within microniches with a range of OM degradation rates and porosities. For all of the modelled scenarios the ion activity product for iron sulphide far exceeds the solubility product, indicating conditions for FeS precipitation in all niches. Those simulations within the $t_{35\%}$ range of 2.5 to 5 days gave comparable concentration ratios of sulphide to iron in solution within the particles to experimentally observed values.

Whilst it was not the aim of this work to specifically investigate processes occurring at microniches in terms of the preservation of OM in the paleo record, it is evident that the modelled data can inform such studies. The model can predict the conditions that result in preferential deposition of precipitates at the edge of microniches. Decreasing porosity, lower $t_{35\%}$ values and increasing OM degradation rates all tend to increase the likelihood that peak iron sulphide precipitation will preferentially occur at the edges of the niche rather than uniformly throughout its volume.

It is likely that both the elevated sulphide and localized zones of FeS will have a significant effect on the diagenesis of trace metals. If microniches comprise a small but significant volume of the oxic and suboxic sediment they may exert an influence on the whole system that would not be predicted if only the bulk sediment was considered. The peak sulphide concentrations modelled here are significantly in excess of all of the critical reaction concentrations observed for molybdenum (these reactions include: co-precipitation with FeS, direct Mo precipitation and direct conversion of molybdate to tetrathiomolybdate). Trace metals available for reaction with sulphide can be supplied by: 1) generation within the particle by release from the degrading OM, 2) inward diffusion from the surrounding sediment, particularly where the Fe/Mn oxides in ambient sediment are the electron acceptors for OM oxidation, or 3) a combination of the two processes. For elements forming sulphide precipitates, the conditions required will evolve quickly (minutes) after the niche is introduced. Over time (hours) the FeS concentration will increase, allowing those elements that can undergo displacement reactions to do so in increasing proportions. As the FeS occurs at most microniches as a halo, the displacement reactions will occur preferentially within this zone.

Supporting information
Additional tables and material, as referred to in the text, are available online at http://www.sciencedirect.com

REFERENCES

Alldredge A.L. and Cohen Y. (1987) Can microscale chemical patches persist in the sea? Microelectrode study of marine snow, fecal pellets. *Science* **235**, 689-691.

Allen R.E. (2002) Role of diffusion-precipitation reactions in authigenic pyritization. *Chem. Geol.* **182**, 461-472.

Alongi D.M., Wattayakorn G., Boyle S., Tirendi F., Payn C. and Dixon P. (2004) Influence of roots and climate on mineral and trace element storage and flux in tropical mangrove soils. *Biogeochemistry* **69**, 105-123.

Bargagli R., Monaci F., Sanchez-Hernandez J. C. and Cateni D. (1998) Biomagnification of mercury in an Antarctic marine coastal food web. *Mar. Ecol.-Prog. Ser.* **169**, 65-76.

Ben-Yaakov S. (1973) pH buffering of pore water of recent anoxic marine sediments. *Limnol. Oceanogr.* **18**, 86-94.

Berg P., Rysgaard S. and Thamdrup B. (2003) Dynamic modeling of early diagenesis and nutrient cycling. A case study in an arctic marine sediment, *Am. J. Sci.* **303**, 905-955.

Berner R.A. (1970) Sedimentary pyrite formation. *Am. J. Sci.* **268**, 1-23.

Berner R.A., (1980) *Early Diagenesis: A Theoretical Approach.* Princeton Univerity Press, Princeton, pp 241.

Brandes J.A., and Devol A.H. (1995) Simultaneous nitrate and oxygen respiration in coastal sediments: evidence for discrete diagenesis. *J. Mar. Res.* **53**, 771-797.

Briggs D.E.G., Bottrell S.H. and Raiswell R. (1991) Pyritization of soft-bodied fossils: Beecher's Trilobite Bed, Upper Ordovician, New York State. *Geology* **19**, 1221-1224.

Briggs D.E.G., Raiswell R., Bottrell S.H., Hatfield D. and Bartels C. (1991) Controls on the pyritization of exceptionally preserved fossils: an analysis of the Lower Devonian Hunsrück Slate of Germany. *Am. J. Sci.* **296**, 633-663.

Bruland K.W., Donat J.R. and Hutchins D.A. (1991) Interactive influences of bioactive trace metals on biological production in oceanic waters. *Limnol. Oceanogr.* **36**, 1555-1577.

Bu-Olayan A.H., Al-Hassan R., Thomas B.V. and Subrahmanyam M.N.V. (2001) Impact of trace metals and nutrients levels on phytoplankton from the Kuwait Coast. *Environ. Int.* **26**, 199-203.

Bostick B.C., Fendorf S. and Helz G.R., (2003) Differential adsorption of molybdate and tetrathiomolybdate on pyrite (FeS$_2$). *Environ. Sci. Technol.* **37**, 285-291.

Boudreau B.P. (1996) A method-of-lines code for carbon and nutrient diagenesis. *Comp. Geosci.* **22**, 479-496.

Burdige D.J., (2006) *Geochemistry of Marine Sediments.* Princeton University Press, Princeton, pp. 609.

Canavan R.W., van Capellen P., Zwolsman J.J.G., van den Berg G.A. and Slomp C.P. (2007) Geochemistry of trace metals in a freshwater sediment : field results and diagenetic modeling. *Sci. Tot. Env.* **381**, 263-279.

Choi J.H., Park S.S., and Jaffe P.R. (2006) Simulating the dynamics of sufur species and zinc in wetland sediments, *Ecol. Model.* **199**, 315-323.

Davison W. (1980) A critical comparison of the measured solubilities of ferrous sulphide in natural waters. *Geochim. Cosmochim. Acta* **44**, 803-808.

Di Toro D.M., Mahony J.D., Scott K.J., Hicks M.B., Mayer S.M. and Redmond M.S. (1990) Toxicity of cadmium in sediment − the role of acid volatile sulphide. *Environ. Toxicol. Chem.* **9**, 1487-1502.

Di Toro D.M., Mahony J.D., Hansen D.J., Scott K.J., Carlson A.R. and Ankley G.T. (1992) Acid volatile sulphide predicts the acute toxicity of cadmium and nickel in sediments. *Environ. Sci. Technol.* **26**, 96-101.

Douglas G.B. and Adeney J.A. (2000) Diagenetic cycling of trace elements in the bottom sediments of the Swan River Estuary, Western Australia. *Appl. Geochem.* **15**, 551-566.

Druschel G.K., Labrenz M., Thomsen-Ebert T., Fowle D.A. and Banfield J.F. (2002) Geochemical modeling of ZnS in biofilms: an example of ore depositional processes. *Econ. Geol.* **97**, 1319-1329.

Ebihara N., Uchida T., Ogura H. and Oguma K. (2006) Determination of metal elements in marine planktons after pressurized acid decomposition. *Bunseki Kagaku* **55**, 855-861. (In Japanese with abstract, figures and tables in English).

Erickson B.E. and Helz G.R. (2000) Molybdenum (VI) speciation in sulfidic waters: stability and lability of thiomolybdates. *Geochim. Cosmochim. Acta* **64**, 1149-1158.

Fisher N.S., Nolan C.V. and Fowler S.W. (1991) Scavenging and retention of metals by zooplankton fecal pellets and marine snow. *Deep Sea Res.* **38**, 1261-1275.

Fossing H., Berg P., Thamdrup B., Rysgaard S., Sørensen H.M. and Nielsen K. (2002) Ilt- og næringsstoffluxmodel for Århus Bugt og Mariager Fjord - *Faglig rapport fra DMU nr. 416*, Danmarks Miljøundersøgelser, pp72.

Fossing H., Berg P., Thamdrup B., Rysgaard S., Sørensen H.M. and Nielsen K. (2004) A model set-up for an oxygen and nutrient flux model for Aarhus Bay (Denmark). *NERI Technical Report No. 483*. National Environmental Research Institute, Denmark, pp65.

Froelich P.N., Klinkhammer G.P., Bender M.L., Luedtke G.R., Heath G.R., Cullen D. and Dauphin P. (1979) Early oxidation of organic matter in pelagic sediments of the eastern equatorial Atlantic: suboxic diagenesis. *Geochim. Cosmochim. Acta* **43**, 1075-1090.

Helz G.R., Vorlicek T.P. and Kahn M.D. (2004) Molybdenum scavenging by monosulfide. *Environ. Sci. Technol.* **38**, 4263-4268.

Ho T.-Y., Quigg A., Finkel Z.V., Milligan A.J., Wyman K., Falkowski P.J. and Morel F.M.M. (2003) The elemental composition of some marine phytoplankton. *J. Phycol.* **39**, 1145-1159.

Huerta-Diaz M.A. and Morse J.W. (1990) A quantitative method for determination of trace metal concentrations in sedimentary pyrite. *Mar. Chem.* **29**, 119-144.

Huerta-Diaz M.A. and Morse J.W. (1992) Pyritization of trace metals in anoxic sediments. *Geochim. Cosmochim. Acta* **56**, 2681-2702.

Huerta-Diaz M.A., Tessier A. and Carignan R. (1998) Geochemistry of trace metals associated with reduced sulfur in freshwater sediments. *Appl. Geochem.* **13**, 213-233.

Jahnke R. (1985) A model of microenvironments in deep-sea sediments: formation and effects on porewater profiles. *Limnol. Oceanogr.* **30**, 956-965.

Jørgensen B.B. (1977) Bacterial sulfate reduction within reduced microniches of oxidized marine-sediments. *Mar. Biol.* **41**, 7-17.

Lee B.-G. and Fisher N.S. (1992) Decomposition and release of elements from zooplankton debris. *Mar. Ecol. Prog. Ser.* **88**, 117-128.

Martin J.H. and Knauer G. A. (1973) The elemental composition of plankton. *Geochim. Cosmochim. Acta* **37**, 1639-1653.

Martin J.H., Bruland K.W. and Broenkow W.W. (1976) Cadmium transport in the California Current. In: *Marine pollutant transfer* (eds. H.L. Windom and R.A. Duce). Lexington Books, Lexington. pp. 159-184.

Michel P., Boutier B., Herbland A., Averty B., Artigas L.F., Auger D. and Chartier E. (1998) Behaviour of arsenic on the continental shelf off the Gironde estuary: role of phytoplankton in vertical fluxes during spring bloom conditions. *Oceanologica Acta* **21**, 325-333.

Millero F.J. and Schreiber D.R. (1982) Use of the ion pairing model to estimate activity coefficients of the ionic components of natural waters. *Am. J. Sci.* **282**, 1508-1540.

Morse J.W. and Luther G.W. (1999) Chemical influences on trace metal-sulphide interactions in anoxic sediments. *Geochim. Cosmochim. Acta* **63**, 3373-3378.

Morse J.W. and Eldridge P.M. (2007) A non-steady state diagenetic model for changes in sediment biogeochemistry in response to seasonally hypoxic/anoxic conditions in the "dead zone" of the Louisiana shelf. *Mar. Chem.* **106**, 239-255.

Motelica-Heino M., Naylor C., Zhang H. and Davison W. (2003) Simultaneous release of metals and sulfide in lacustrine sediment. *Environ. Sci. Technol.* **37**, 4374-4381.

Otero X.L. and Macias F. (2003) Spatial variation in pyritization of trace metals in salt-marsh soils. *Biogeochemistry* **62**, 59-86.

Raiswell R. (1993) Kinetic controls on depth variations in localised pyrite formation. *Chem. Geol.* **107**, 467-469.

Raiswell R., Whaler K., Dean S., Coleman M.L. and Briggs D.E.G. (1993) A simple three-dimensional model of diffusion-with-precipitation applied to localised pyrite formation in framboids, fossils and detrital iron minerals. *Mar. Geol.* **113**, 89-100.

Raiswell R., Newton R., Bottrell S.H., Coburn P.M., Briggs D.E.G., Bond D.P.G. and Poulton S.W. (2008) Turbidite depositional influences on the diagenesis of Beecher's Trilobite Bed and the Hunsrück Slate; sites of soft tissue pyritization. *Am. J. Sci.* **308**, 105-129.

Rysgaard S., Thamdrup B., Risgaard-Petersen N., Fossing H., Berg P., Christensen P.B. and Dalsgaard T. (1998) Seasonal carbon and nitrogen mineralization in a high-Arctic coastal marine sediment, Young Sound, Northeast Greenland. *Mar. Ecol. Prog. Ser.* **179**, 262-276.

Sagemann J., Bale S.J., Briggs D.E.G. and Parkes R.J. (1999) Controls on the formation of authigenic minerals in association with decaying organic matter: an experimental approach. *Geochim. Cosmochim. Acta* **63**, 1083-1095.

Sell K.S. and Morse J.W. (2006) Dissolved Fe^{2+} and $\sum H_2S$ behavior in sediments seasonally overlain by hypoxic-to-anoxic waters as determined by CSV microelectrodes. *Aquatic Geochemistry* **12**, 179–198.

Sochaczewski Ł., Stockdale A., Davison W., Tych W. and Zhang H. (2008) A three-dimensional reactive transport model for sediments, incorporating microniches. *Environ. Chem.* **5**, 218-225.

Stockdale A., Davison W. and Zhang H. (revisions submitted) Micro-scale biogeochemical heterogeneity in sediments: a review of available technology and observed evidence. *Earth-Sci. Rev.*

Stockdale A., Davison W. and Zhang H. (2008a) High-resolution two-dimensional quantitative analysis of phosphorus, vanadium & arsenic, and qualitative analysis of sulphide, in a freshwater sediment. *Environ. Chem.* **5**, 143-149.

Tessier A., Fortin D., Belzile N., DeVitre R.R. and Leppard G.G. (1996) Metal sorption to diagenetic iron and manganese oxyhydroxides and associated organic matter: narrowing the gap between field and laboratory measurements. *Geochim. Cosmochim. Acta* **60**, 387-404.

Van Cappellen P., Galliard J.-F. and Rabouille C. (1993) Biogeochemical transformations in sediments: kinetic models of early diagenesis. In *Interactions of C, N, P and S Biogeochemical Cycles and Global Change* (eds. R. Woolast, F.T. Mackenzie and L. Chou). Springer-Verlag, Berlin. pp 401-445.

Wallschläger D. and Stadey C.J. (2007) Determination of (oxy)thioarsenates in sulphidic waters, *Anal. Chem.* **79**, 3873-3880.

Wang Y. and van Cappellen P. (1996) A multicomponent reactive transport model of early diagenesis: Application to redox cycling in coastal marine sediments. *Geochim. Cosmochim. Acta* **60**, 2993-3014.

Watling L. (1988) Small-scale features of marine sediments and their importance to the study of deposit-feeding. *Mar. Ecol.-Prog. Ser.* **47**, 135-144.

Westrich J.T. and Berner R.A. (1984) The role of sedimentary organic-matter in bacterial sulfate reduction – the G model tested. *Limnol. Oceanogr.* **29**, 236-249.

Widerlund A. and Davison W. (2007) Size and density distribution of sulfide-producing microniches in lake sediments. *Environ. Sci. Technol.* **41**, 8044-8049.

Wijsman J.W.M., Herman P.M.J., Middelburg J.J. and Soetaert K. (2002) A model for early diagenetic processes in sediments of the continental shelf of the Black Sea. *Estuarine Coastal Shelf Sci.* **54**, 403-421.

Zheng Y., Anderson R.F., van Gleen A. and Kuwabara J. (2000) Authigenic molybdenum formation in marine sediments: a link to porewater sulphide in the Santa Barbara Basin. *Geochim, Cosmochim. Acta* **64**, 4165-4178.

Zhu Q.Z., Aller R.C. and Fan Y.Z. (2006) Two-dimensional pH distributions and dynamics in bioturbated marine sediments. *Geochim. Cosmochim. Acta* **70**, 4933-4949.

Sulphide evolution from faecal pellets and other microniches within sub oxic surface sediment: The effects on the geochemistry of iron and trace elements

Anthony Stockdale, William Davison*, Hao Zhang

Department of Environmental Science, Lancaster Environment Centre (LEC), Lancaster University, Lancaster LA1 4YQ, United Kingdom

*Corresponding author

Fax: +44-1524-93985; e-mail: w.davison@lancaster.ac.uk

Supporting Information

Additional tables

Table S1. Model parameters.

Parameter	Value	Reference
Domain	x,y,z: 0.7, 0.7, 1.0 cm	
Resolution[a]	0.052	
Bulk porosity (entered as finite values in the 3d model)	$\varphi = 0.832$	(1)
Tortuosity option	Iversen- Jørgensen. n = 2.79	
Diffusion coefficients at 10ºC NH_4^-	13.7×10^{-6} cm^2 s^{-1}	(1)
SO_4^{2-}	7.22×10^{-6} cm^2 s^{-1}	(1)
$\sum H_2S$	11.8×10^{-6} cm^2 s^{-1}	(1)
Mn	4.57×10^{-6} cm^2 s^{-1}	(2)
Fe	4.48×10^{-6} cm^2 s^{-1}	(2)
Boundary conditions[b]		
U = Upper (0.67 cm below SWI)		
L = Lower (1.67 cm below SWI)		
$[O_2]$	U & L 0 µM	(1)
$[NO_3^-]$	U & L 0 µM	(1)
$[NH_4^-]$	U 36 µM; L 83 µM	(1)
$[Fe^{2+}]$	U 56 µM; L 91 µM	(1)
$[Mn^{2+}]$	U 70 µM; L 60 µM	(1)
$[SO_4^{2-}]$	U & L 2000 µM	(1)
$[\sum H_2S]$	U & L 0 µM	(1)
Limiting concentrations (Niche = 2% of bulk value) $[MnO_2]$	Bulk 1.02×10^5 µM	(1)
	Niche 2.04×10^3 µM	
$[FeOOH]$	Bulk 2.04×10^5 µM	(1)
	Niche 4.08×10^3 µM	
Rate constants k_{OM-s}	1.2×10^{-8} s^{-1}	(1)
k_{OM-f}	See Figure 2	
k_6	2.5×10^{-6} µM^{-1} s^{-1}	(1)
k_7	1.5×10^{-5} µM^{-1} s^{-1}	(1)
k_8	5.0×10^{-4} µM^{-1} s^{-1}	(1)
k_9	$1.7. \times 10^{-8}$ µM^{-1} s^{-1}	(1)
k_{10}	2.0×10^{-8} µM^{-1} s^{-1}	(1)
k_{11}	3.0×10^{-9} µM^{-1} s^{-1}	(1)
k_{12}	7.5×10^{-7} µM^{-1} s^{-1}	(1)
k_{13}	6.0×10^{-7} µM^{-1} s^{-1}	(1)
k_{14}	5.0×10^{-5} µM^{-1} s^{-1}	(1)

(1) Fossing et al (2002, 2004). (2) Li and Gregory (1974). [a]See Sochaczewski et al (2008) for a full description of the resolution and mesh density. [b]Boundaries are based on the 1D profiles from (1).

Table S2. Trace metal fractions associated with Fe and Mn oxides used in calculations for Table 4 (values are the Tessier et al, 1992, values divided by 2.5. See main manuscript for explanation of this adjustment.

Metal	MnO$_2$	FeOOH
	(mol mol^{-1})	
Ni	5.52×10^{-2}	6.12×10^{-3}
Cu	4.40×10^{-3}	2.20×10^{-3}
Zn	4.20×10^{-3}	2.00×10^{-3}
Cd	5.12×10^{-5}	1.36×10^{-5}
Pb	1.12×10^{-4}	2.00×10^{-4}

Zinc-sulphide modelling

Whilst modelling of general trace metal-sulphide interactions is limited, several studies have attempted to model zinc-sulphide reactions. Druschel et al (2002) modelled zinc sulphide (ZnS) formation (precipitation) in sulphate reducing biofilms within flooded mine tunnels under conditions where the biofilm is exposed to a continuous flow of water containing high dissolved zinc concentrations (~1.4 ppm). Under these conditions it is suggested that, provided Zn^{2+} is introduced faster than sulphide is generated, ZnS precipitation should occur to the exclusion of FeS. Such conditions will not exist at sedimentary microniches where Fe^{2+} concentrations will be orders of magnitude higher than Zn^{2+} and where sulphide concentrations have been observed to be over 40 times higher than those of Fe^{2+} (Motelica-Heino et al, 2003).

Canavan et al (2007) modelled (and measured) trace metal behaviour in a freshwater sediment using a two reaction approach to ZnS formation. The first was a precipitation reaction (Eq. S1), where $k_{ZnS-precip}$ is a rate constant (3.17×10^{-18} mol g^{-1} s^{-1}) and $K_{ZnS(sp)}$ is the equilibrium constant ($10^{-9.02}$). Both constants were used as model fitting parameters and this reaction was not allowed to proceed when ZnS was

undersaturated. This reaction is analogous to the iron sulphide precipitation/dissolution reactions used by van Cappellen et al (1993).

$$ZnS_{precip} = k_{ZnS\text{-}precip}\left(\frac{[Zn^{2+}][HS^-]}{[H^+]K_{ZnS(sp)}}-1\right) \qquad (S1)$$

Secondly a displacement reaction is used (Eq. S2).

$$Zn^{2+} + FeS \xrightarrow{\ k_{disp}\ } ZnS + Fe^{2+} \qquad (S2)$$
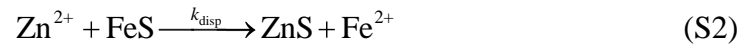
Canavan et al (2007) assumed the rate constant for Equation S2 had first order kinetics (first order for Zn^{2+}) and this value was also used as a fitting parameter. Experimental evidence for reactions that displace iron has been reported (Di Toro et al, 1992; and references therein).

Choi et al (2006) modelled sulphur dynamics in a vegetated wetland sediment and assumed Equation S2 was the only ZnS formation mechanism. They used a second order rate constant for k_{disp}. The rate constant was assumed to be equal to the constant for the formation of FeS from Fe^{2+} and $\sum S(II)$. Using this single reaction approach may not be appropriate for modelling zinc/sulphide reactions at fresh microniches, as it requires FeS to form prior to ZnS, which contradicts the reported faster water exchange kinetics of Zn^{2+} compared to Fe^{2+} (Morse and Luther, 1999). These modelling examples indicate the complexity of modelling trace metal dynamics in sulphidic sediments.

Additional references

Li, Y.H., Gregory, S., 1974. Diffusion of ions in sea water and deep sea sediments. Geochimica et Cosmochimica Acta, 38,703-714.

4   Conclusions

The principal aim of this thesis was to further our understanding of processes occurring at microniches. The objective was carried out by experimental work using DGT to measure concentrations of anions at a sulphidic niche in sediments and by modelling the sulphide evolution and associated geochemistry at an idealised spherical niche within sediment, using a comprehensive data set.

A review of previous microniche research has shown that our understanding of sedimentary diagenesis has been somewhat oversimplified by analysis at a larger, spatially averaged, scale and that the lack of congruent analysis makes it difficult to interpret these data in terms of specific geochemical processes. Using a new binding phase that allows co-analysis of sulphide, phosphate and the trace anions, arsenate and vanadate, has shown that depletions in anions occur at a microniche of elevated sulphide. Phosphate uptake associated with elevated activity of sulphate reducing bacteria has been demonstrated. Further work is required to determine if bacterial uptake, use by bacteria as an electron acceptor, reduction by sulphide and subsequent scavenging, or other processes are responsible for the observed depletions associated with sulphide production.

Using a three-dimensional diagenetic model, simulation of the hypothetical cases of microniches in the near surface sediment showed that, for the conditions selected, sulphide was readily generated, provided the microniche diameter was greater than 1 mm. In scenarios that were shown to be relevant to experimental observations reported in the literature, the behaviour of sulphide and iron within microniches with a range of degradation rates and porosities was modelled. For all of the modelled

scenarios, the ion activity product for iron sulphide far exceed the solubility product, indicating conditions for FeS precipitation in all niches. Decreasing porosity, lowering niche life-times and increasing OM degradation rates all tend to increase the likelihood that peak iron sulphide precipitation will preferentially occur at the edges of the niche rather than uniformly throughout its volume. It is likely that both the elevated sulphide and localized zones of FeS will have a significant effect on the diagenesis of trace metals. For elements that can form sulphide precipitates, the conditions required will evolve quickly (minutes) after the niche is introduced. Over time (hours) the FeS concentration will increase and those elements that can undergo displacement reactions will do so increasingly, as the rate of displacement is related to the FeS concentration.

5   The wider significance of microniche processes and future priorities

Research into the geochemistry and significance of microniches has, to date, been very piecemeal, with a tendency to have single unrelated research papers, often separated by several years and covering different sedimentary environments. This thesis has reviewed much of this body of work and includes three research papers dedicated to microniche geochemistry. Given that this information is collated into one volume here, it is worthwhile additionally providing an opinion on the possible rationales for this research, and suggestions for the key areas of future studies. As this synthesis includes speculative assessments of numerous studies, it is included at the end of all investigative material to avoid any conflict with the thesis conclusions.

Firstly it is important to stress again that bioturbation is likely to be an important prerequisite for microniche formation, as it accounts for their distribution. In non-

bioturbated environments, such as in euxinic sediment with varve deposits, clear horizontally homogeneous patterns exist that can be explained by considering the system in one-dimension. One of the key questions when considering the significance of microniches on other aspects of geochemistry is: are they important to long-term processes such as mineral formation, particularly trace element sulphides, and do we need to consider this when assessing paleoredox proxies? Clearly, in microniches where no sulphide evolution exists, changes will occur to local profiles of oxidants and OM degradation products, such as NH_4^+ and CO_2. However, trace element release under these circumstances is unlikely to be under conditions where they are irreversibly immobilised locally or permanently converted to the mineral phase.

Table 1 highlights the characteristics of both sediments and microniches that may effect the ultimate significance of microniche processes. Of these characteristics, the most important in terms of trace metal sulphide formation will be those that allow for sulphide evolution within the niche, together with those that control the potential reversibility of the metal sulphide formation reactions.

Once a niche is no longer generating sulphide internally, and where ambient conditions are not sulphidic, the localized system will become substantially undersaturated for metal sulphides. The loss of precipitated trace elements (e.g. ZnS) and bound anionic sulphide species (e.g. $\equiv MoS_4$) from a niche will be controlled by a number of factors. 1) The rate constant of the dissolution reaction. 2) Factors that may inhibit reverse reactions such as interactions with other solid phases. 3) The duration of the undersaturation event (i.e. translocation of the microniche by the actions of biota).

For many trace element sulphides it is unlikely that the reactions are fully reversible, as conditions 1) to 3) will not always be favourable.

5.1 Improving model predictions and use of organic matter degradation rates

Modelling of sediment systems in 1D generally utilises a Multi-G approach. By allowing the specification of a near-surface, fast reacting pool of OM imposed onto a more evenly distributed slow reacting pool, more accurate model results have been achieved for solute distributions. However, the fast reacting pool is considered as horizontally homogeneous and thus a universal rate constant is applied. Consider a situation where this pool consists entirely of microniches, with a depth distribution of decreasing particle density away from the sediment water interface. It would be reasonable to expect some of the niches to exist below the O_2 and NO_3^- penetration depths, and that some particles within these upper redox zones will have conditions whereby these oxidants become limiting. This may result in the following effects. Firstly, sulphide will be produced in zones where it is not expected. Often models use fixed constants for biological processes such as biodiffusion or irrigation to explain such observations. The existence of microniches requires an additional consideration. Secondly, 1D models do not take into account that some of the fast reacting OM may be oxidised by electron acceptors other than O_2 and NO_3^-. For the profiles of O_2 and NO_3^- measured in 1D, to be comparable to those modelled in 3D environment, requires that either, the pool size of fast reacting OM is increased, or that the reaction rate of OM (within these redox zones) is increased. These adjustments are required in order to balance the O_2 and NO_3^- consumption rates and therefore to maintain their vertical profiles.

5.2   Priorities for future work

In order to gain a better understanding of microniche process and their significance in terms of trace element sulphide sinks, there are, in my view, three key questions to be addressed.

1.   The distribution and translocation of microniches needs to be investigated. Use of planar probes such as DGT and planar optodes may encourage preferential burrowing adjacent to the device. This can be an advantage when studying the actual geochemical processes. However, it cannot give accurate quantitative data for the entire volume of sediment due to this effect. Other techniques need to be employed to determine actual distributions of niches. Gridded deployment of needle electrodes for analysis of solutes such as sulphide, may yield some useful information. Although, the limitations of these types of probes, as discussed in Paper I, will apply.

2.   In sulphate reducing microniches the effect of the pH decrease within the niche needs to be quantified. The change in pH will reduce the degree of saturation of the trace element sulphides and thus the rate at which precipitation occurs. In microniches at locations where sulphide does not evolve, e.g. in the oxic zone, this pH effect may influence other mineral phases such as carbonates.

3.   The relative reversibility of trace element sulphide formation is an important consideration when assessing the significance of microniches, and good progress has been made in understanding how these processes are controlled for molybdenum. Further data is required for other trace elements and additional effects of processes such as surface adsorption or formation of organic coatings need to be investigated.

6 Consolidated references

Alldredge, A.L., 1979. The chemical composition of macroscopic aggregates in two neretic seas. Limnology and Oceanography, 24, 855-866.

Alldredge, A.L., Cohen, Y., 1987. Can microscale chemical patches persist in the sea? Microelectrode study of marine snow, fecal pellets. Science, 235, 689-691.

Alldredge, A.L., Cole, J.J., Caron, D.A., 1986. Production of heterotrophic bacteria inhabiting macroscopic organic aggregates (marine snow) from surface waters. Limnology and Oceanography, 31, 68-78.

Allen, R.E., 2002. Role of diffusion-precipitation reactions in authigenic pyritization. Chemical Geology, 182, 461-472.

Aller, R.C., 1982. The effects of macrobenthos of chemical properties of marine sediment and overlying water. In: McCall, P.L., Tevesz, M.J.S., (Eds.), Animal-Sediment Relations, Plenum Press, New York, pp. 53-102.

Aller, R.C., 1983. The importance of the diffusive permeability of animal burrow linings in determining marine sediment chemistry. Journal of Marine Research, 41, 299-322.

Aller, R.C., 1988. Benthic fauna and biogeochemical processes in marine sediments: microbial activities and fluxes. In: Blackburn, T.H., Sorensen, J., (Eds.), Nitrogen Cycling in Coastal Marine Environments, John Wiley and Sons, Chichester, pp. 301-338.

Aller, R.C., 1994. Bioturbation and remineralization of sedimentary organic matter: effects of redox oscillation. Chemical Geology, 114, 331-345.

Aller, R.C., 2001. Transport and reactions in the bioirrigated zone. In: Boudreau, B.P., Jørgensen, B.B., (Eds.), The Benthic Boundary Layer: Transport Processes and Biogeochemistry, Oxford University Press, Oxford, pp. 269-301.

Aller, R.C., Yingst. J.Y., 1978. Biogeochemistry of tube-dwellings: A study of the sedentary polychaete *Amphitrite ornate* (Leidy). Journal of Marine Research, 36, 201-254.

Aller, R.C., Mackin, J.E., 1989. Open-incubation, diffusion methods for measuring solute reaction rates in sediments. Journal of Marine Research, 47, 411-440.

Aller, R.C., Yingst. J.Y., Kemp, P.F., 2001. Effects of particle and solute transport on rates and extent of remineralization in bioturbated sediment. In: Aller,

J.Y., Woodin, S.A., Aller, R.C., (Eds.), Organism-Sediment Interactions, University of South Carolina Press, Columbia, pp. 315-333.

Alongi, D.M., Wattayakorn, G., Boyle, S., Tirendi, F., Payn, C., Dixon, P., 2004. Influence of roots and climate on mineral and trace element storage and flux in tropical mangrove soils. Biogeochemistry, 69, 105-123.

Amao, Y., 2003. Probes and polymers for optical sensing of oxygen. Microchimica Acta, 143, 1-12.

Anschutz, P., Sundby, B., Lefrancois, L., Luther, G.W., Mucci, A., 2000. Interactions between metal oxides and species of nitrogen and iodine in bioturbated marine sediments. Geochimica et Cosmochimica Acta, 64, 2751-2763.

Axelsson, V., Händel, S.K., 1972. X-radiography of unextruded sediment cores. Geografiska Annaler, 54A: 1, 34-37.

Bargagli, R., Monaci, F., Sanchez-Hernandez, J. C., Cateni, D., 1998. Biomagnification of mercury in an Antarctic marine coastal food web. Marine Ecology-Progress Series, 169, 65-76.

Bell, J.M.L., Philp, J.C., Kuyukina, M.S., Ivshina, I.B., Dunbar, S.A., Cunningham, C.J., Anderson, P., 2004. Methods evaluating vanadium tolerance in bacteria isolated from crude oil contaminated land. Journal of Microbiological Methods, 58, 87-100.

Ben-Yaakov, S., 1973. pH buffering of pore water of recent anoxic marine sediments. Limnology and Oceanography, 18, 86-94.

Berg, P., Rysgaard, S., Thamdrup, B., 2003. Dynamic modeling of early diagenesis and nutrient cycling. A case study in an arctic marine sediment. American Journal of Science, 303, 905-955.

Berner, R.A., 1970. Sedimentary pyrite formation. American Journal of Science, 268, 1-23.

Berner, R.A., 1980. Early Diagenesis: A Theoretical Approach. Princeton University Press, Princeton, pp. 241.

Bernhard, J.M., Bowser, S.S., 1996. Novel epifluorescence microscopy method to determine life position of foraminifera in sediments. Journal of Micropalaeontology, 15, 68-68.

Bernhard, J.M., Visscher, P.T., Bowser, S.S., 2003. Submillimeter life positions of bacteria, protists, and metazoans in laminated sediments of the Santa Barbara Basin. Limnology and Oceanography, 48, 813-828.

Balistrieri, L., Murray, J., Paul, B., 1994. The geochemical cycling of trace elements in a biogenic meromictic lake. Geochimica et Cosmochimica Acta, 58, 3993–4008.

Blomqvist, S., 1985. Reliability of core sampling of soft bottom sediment-an in situ study. Sedimentology, 32, 605-612.

Blomqvist, S., 1991. Quantitative sampling of soft-bottom sediments: problems and solutions. Marine Ecology Progress Series, 72, 295-304.

Bloomfield, C., Kelso, W.I., 1973. The mobilization and fixation of molybdenum, vanadium and uranium by decomposing organic matter. Journal of Soil Science, 24, 368-379.

Bostick, B.C., Fendorf, S., Helz, G.R., 2003. Differential adsorption of molybdate and tetrathiomolybdate on pyrite (FeS_2). Environmental Science and Technology, 37, 285-291.

Boudreau, B.P., 1996. A method-of-lines code for carbon and nutrient diagenesis. Computers and Geosciences, 22, 479-496.

Boudreau, B.P., 1997. Diagenetic Models and their Implementation. Springer, Berlin, pp. 414.

Boudreau, B.P., Meysman, F.J.R., 2006. Predicted tortuosity of muds. Geology, 34, 693-696.

Brandes, J.A., Devol, A.H., 1995. Simultaneous nitrate and oxygen respiration in coastal sediments: evidence for discrete diagenesis. Journal of Marine Research, 53, 771-797.

Brendel, P.J., Luther, G.W., 1995. Development of a gold amalgam voltammetric microelectrode for the determination of dissolved Fe, Mn, O_2, and S(-II) in porewaters of marine and freshwater sediments. Environmental Science and Technology, 29, 751-761.

Briggs, D.E.G., Bottrell, S.H., Raiswell R., 1991. Pyritization of soft-bodied fossils: Beecher's Trilobite Bed, Upper Ordovician, New York State. Geology, 19, 1221-1224.

Briggs, D.E.G., Raiswell, R., Bottrell, S.H., Hatfield, D., Bartels, C., 1991. Controls on the pyritization of exceptionally preserved fossils: an analysis of the Lower Devonian Hunsrück Slate of Germany. American Journal of Science, 296, 633-663.

Bruland K.W., Donat, J.R., Hutchins, D.A., 1991. Interactive influences of bioactive trace metals on biological production in oceanic waters. Limnology and Oceanography, 36, 1555-1577.

Buchanan, J.Y., 1890. On the occurrence of sulphur in marine muds and nodules, and its bearing on their mode of formation. Proceedings of Royal Society of Edinburgh, 18, 17-39.

Buckland, W., 1835. On the discovery of coprolites, or fossil faeces, in the Lias at Lyme Regis, and in other formations. Transaction of the Geological Society, London, 2, 223-236.

Buffle, J., Horvai, G., (Eds.), 2000. In Situ Monitoring of Aquatic Systems: Chemical Analysis and Speciation. John Wiley and Sons, Chichester, pp. 642.

Bu-Olayan, A.H., Al-Hassan, R., Thomas, B.V., Subrahmanyam, M.N.V., 2001. Impact of trace metals and nutrients levels on phytoplankton from the Kuwait Coast. Environment International, 26, 199-203.

Burdige, D.J., 2006. Geochemistry of Marine Sediments. Princeton University Press, Princeton, pp. 609.

Cai, W.J., Reimers, C.E., Shaw, T., 1995. Microelectrode studies of organic-carbon degradation and calcite dissolution at a California continental rise site. Geochimica et Cosmochimica Acta, 59, 497-511.

Cai, W.J., Zhao, P.S., Wang, Y.C., 2000. pH and pCO$_2$ microelectrode measurements and the diffusive behavior of carbon dioxide species in coastal marine sediments. Marine Chemistry, 70, 133-148.

Calvert, S.E., Veevers, J.J., 1962. Minor structures of unconsolidated marine sediments revealed by x-radiography. Sedimentology, 1, 287-295.

Canavan, R.W., van Capellen, P., Zwolsman, J.J.G., van den Berg, G.A., Slomp, C.P., 2007. Geochemistry of trace metals in a freshwater sediment : field results and diagenetic modeling. Science of the Total Environment, 381, 263-279.

Cardenas, M.B., Wilson, J.L., 2006. The influence of ambient groundwater discharge on exchange zones induced by current-bedform interactions. Journal of Hydrology, 331, 103-109.

Cardenas, M.B., Wilson, J.L, 2007. Dunes, turbulent eddies, and interfacial exchange with permeable sediments. Water Resources Research, 43, W08412, doi:10.1029/2006WR005787

Cardenas, M.B., Wilson, J.L., 2007. Effects of current-bed form induced fluid flow on the thermal regime of sediments. Water Resources Research, 43, W08431, doi:10.1029/2006WR005343

Cherry, R.D., Higgo, J.J.W., Fowler, S.W., 1978. Zooplankton fecal pellets and element residence times in the ocean. Nature, 274, 246-248.

Choi, J.H., Park, S.S., Jaffe, P.R., 2006. Simulating the dynamics of sufur species and zinc in wetland sediments, Ecological Modelling, 199, 315-323.

Clark, L.C., Wolf, R., Granger, D., Taylor, Z., 1953. Continuous recording of blood oxygen tensions by polarography. Journal of Applied Physiology, 6, 189-193.

Collier, R.W., 1984. Particulate and dissolved vanadium in the North Pacific Ocean. Nature, 309, 441-444.

Cowen, J.P, Silver, M.W., 1984. The association of iron and manganese with bacteria on marine macroparticulate material. Science, 224, 1340-1342.

Craven, D.B., Jahnke, R.A., Carlucci, A.F., 1986. Fine-scale vertical distributions of microbial biomass and activity in California borderland sediments. Deep-Sea Research Part A, 33, 379-390.

Crusius, J., Calvert, S., Pedersen, T., Sage, D., 1996. Rhenium and molybdenum enrichments in sediments as indicators of oxic, suboxic and sulfidic conditions of deposition. Earth and Planetary Science Letters, 145, 65-78.

Cunningham, J.T., Ramage, G.A., 1888. The *polychaeta sedentaria* of the Firth of Forth. Transactions of the Royal Society of Edinburgh, xxxiii, 635-684.

Dalyell J.G., 1853. The Powers of the Creator Displayed in the Creation, vol. 2, John Van Woorst, London, pp. 327.

Damgaard, L.R., Revsbech, N.P., 1997. A microscale biosensor for methane containing methanotrophic bacteria and an internal oxygen reservoir. Analytical Chemistry, 69, 2262-2267.

Daniele, S., Ciani, I., Baldo, A., Bragato, C., 2007. Application of sphere cap mercury microelectrodes and scanning electrochemical microscopy (SECM) for heavy metal monitoring at solid/solution interfaces. Electroanalysis, 19, 2067-2076.

Dapples, E.C., The effect of macro-organisms upon near-shore marine sediments. Journal of Sedimentary Petrology, 12, 118-126.

Davison, W., 1980. A critical comparison of the measured solubilities of ferrous sulphide in natural waters. Geochimica et Cosmochimica Acta, 44, 803-808.

Davison, W., 1993. Iron and manganese in lakes. Earth-Science Reviews, 34, 119-163.

Davison, W., Zhang, H., 1994. In-situ speciation measurements of trace components in natural-waters using thin-film gels. Nature, 367, 546-548.

Davison, W., Grime, G.W., Morgan, J.A.W., Clarke, K., 1991. Distribution of dissolved iron in sediment pore waters at submillimeter resolution. Nature, 352, 323-325.

Davison, W., Zhang, H., Grime, G.W., 1994. Performance-characteristics of gel probes used for measuring the chemistry of pore waters. Environmental Science and Technology, 28, 1623-1632.

Davison, W., Fones, G.R., Grime, G.W., 1997. Dissolved metals in surface sediment and a microbial mat at 100-μm resolution. Nature, 387, 885-888.

Davison, W., Fones, G., Harper, M., Teasdale, P., Zhang, H., 2000. Dialysis, DET and DGT: in situ diffusional techniques for studying water, sediment and soils. In: Buffle, J., Horvai, G., (Eds.), In Situ Monitoring of Aquatic Systems: Chemical Analysis and Speciation, John Wiley and Sons, Chichester, pp. 495-570.

Davison, W., Zhang, H., Warnken, K.W., 2007. Theory and applications of DGT measurements in soils and sediments. In: Greenwood, R., Mills, G., Vrana, B., (Eds.), Comprehensive Analytical Chemistry, Volume 48, Passive Sampling Techniques in Environmental Monitoring, Elsevier, pp. 353-378.

de Beer, D., Sweerts, J.-P. R.A., van den Heuvel, J.C., 1991. Microelectrode measurement of ammonium profiles in freshwater sediment. FEMS Microbiology Ecology, 86, 1-6.

de Beer, D., van den Heuvel, J.C., Ottengraf, S.P.P., 1993. Microelectrode measurements of the activity distribution in nitrifying bacterial aggregates. Applied And Environmental Microbiology, 59, 573-579.

Devries, C.R., Wang, F.Y., 2003. In situ two-dimensional high-resolution profiling of sulfide in sediment interstitial waters. Environmental Science and Technology, 37, 792-797.

Di Toro, D.M., Mahony, J.D., Hansen, D.J., Scott, K.J., Hicks, M.B., Mayer, S.M., Redmond, M.S., 1990. Toxicity of cadmium in sediment – the role of acid volatile sulphide. Environmental Toxicology and Chemistry, 9, 1487-1502.

Di Toro, D.M., Mahony, J.D., Hansen, D.J., Scott, K.J., Carlson, A.R., Ankley, G.T., 1992. Acid volatile sulfide predicts the acute toxicity of cadmium and nickel in sediments. Environmental Science and Technology, 26, 96-101.

Docekalova, H., Clarisse, O., Salomon, S., Wartel, M., 2002. Use of constrained DET probe for a high-resolution determination of metals and anions distribution in the sediment pore Water. Talanta, 57, 145-155.

Douglas, G.B., Adeney, J.A., 2000. Diagenetic cycling of trace elements in the bottom sediments of the Swan River Estuary, Western Australia. Applied Geochemistry 15, 551-566.

Druschel, G.K., Labrenz, M., Thomsen-Ebert, T., Fowle, D.A., Banfield, J.F., 2002. Geochemical modeling of ZnS in biofilms: an example of ore depositional processes. Economic Geology, 97, 1319-1329.

Dufour, S.C., Desrosiers, G., Long, B., Lajeunesse, P., Gagnoud, M., Labrie, J., Archambault, P., Stora, G., 2005. A new method for three-dimensional visualization and quantification of biogenic structures in aquatic sediments using axial tomodensitometry. Limnology and Oceanography – Methods, 3, 372-380.

Ebihara, N., Uchida, T., Ogura, H., Oguma, K., 2006. Determination of metal elements in marine planktons after pressurized acid decomposition. Bunseki Kagaku, 55, (11), 855-861. (In Japanese with abstract, figures and tables in English).

Eggleton, J., Thomas, K.V., 2004. A review of factors affecting the release and bioavailability of contaminants during sediment disturbance events. Environment International, 30, 973-980.

Emerson, S., Grundmanis, V., Graham, D., 1982. Carbonate chemistry in marine porewaters: MANOP sites C and S. Earth and Planetary Science Letters, 61, 220-232.

Emery, K.O., Rittenberg, S.C., 1952. Early diagenesis of California Basin sediments in relation to origin of oil. Bulletin of the American Association of Petroleum Geologists, 36, 735-806.

Engesgaard, P., Kipp, K.L., 1992. A geochemical transport model for redox controlled movement of mineral fronts in groundwater flow systems: A case of nitrate removal by oxidation of pyrite. Water Resources Research, 28, 2829-2843.

Erickson, B.E., Helz, G.R., 2000. Molybdenum (VI) speciation in sulfidic waters: stability and lability of thiomolybdates. Geochimica et Cosmochimica Acta, 64, 1149-1158.

Ernstberger, H., Davison, W., Zhang, H., Tye, A., Young, S., 2002. Measurement and dynamic modeling of trace metal mobilisation in soils using DGT and DIFS. Environmental Science and Technology, 36, 349-354.

Ernstberger, H., Zhang, H., Tye, A., Young, S., Davison, W., 2005. Desorption kinetics of Cd, Zn and Ni measured in soils by DGT. Environmental Science and Technology, 39, 1591-1597.

Fenchel, T., 1996. Worm burrows and oxic microniches in marine sediments. 1. Spatial and temporal scales. Marine Biology, 127, 289-295.

Fenchel, T., 1996. Worm burrows and oxic microniches in marine sediments. 2. Distribution patterns of ciliated protozoa. Marine Biology, 127, 297-301.

Fenchel, T., Glud, R.N., 2000. Benthic primary production and O_2-CO_2 dynamics in a shallow-water sediment: Spatial and temporal heterogeneity. Ophelia, 53, 159-171.

Fisher, N.S., Nolan, C.V., Fowler, S.W., 1991. Scavenging and retention of metals by zooplankton fecal pellets and marine snow. Deep Sea Research, 38, 1261-1275.

Fones, G.R., Davison, W., Grime, G.W., 1988. Development of constrained DET for measurements of dissolved iron in surface sediments at sub-mm resolution. Science of the Total Environment, 221, 127-137.

Fones, G.R., Davison, W., Holby, O., Jørgensen, B.B., Thamdrup, B., 2001. High-resolution metal gradients measured by in situ DGT/DET deployment in Black Sea sediments using an autonomous benthic lander. Limnology and Oceanography, 46, 982-988.

Fones, G., Davison, W., Hamilton-Taylor, J., 2004. The fine-scale remobilization of metals in the surface sediment of the North-East Atlantic. Continental Shelf Research, 24, 1485–1504.

Fones, G.R., Davison, W., Hamilton-Taylor, J., 2004. The fine-scale remobilization of metals in the surface sediment of the North-East Atlantic. Continental Shelf Research, 24, 1485-1504.

Fossing, H., Berg, P., Thamdrup, B., Rysgaard, S., Sørensen, H.M., Nielsen, K., 2002. Ilt- og næringsstoffluxmodel for Århus Bugt og Mariager Fjord - Faglig rapport fra DMU nr. 416, Danmarks Miljøundersøgelser, pp. 72.

Fossing, H., Berg, P., Thamdrup, B., Rysgaard, S., Sørensen, H.M., Nielsen, K., 2004. A model set-up for an oxygen and nutrient flux model for Aarhus Bay

(Denmark). NERI Technical Report No. 483, National Environmental Research Institute, Denmark, pp. 65.

Fox, P.M., Doner, H.E., 2003. Accumulation, release, and solubility of arsenic, molybdenum and vanadium in wetland sediments. Journal of Environmental Quality, 32, 2428-2435.

Frederiksen, M.S., Glud, R.N., 2006. Oxygen dynamics in the rhizosphere of *Zostera marina*: a two-dimensional planar optode study. Limnology and Oceanography, 51, 1072-1083.

Froelich, P.N., Klinkhammer, G.P., Bender, M.L., Luedtke, G.R., Heath, G.R., Cullen, D., Dauphin, P., 1979. Early oxidation of organic matter in pelagic sediments of the eastern equatorial Atlantic: suboxic diagenesis. Geochimica et Cosmochimica Acta, 43, 1075-1090.

Garmo, Ø.A., Davison, W., Zhang, H., In press. Effects of diffusion layer binding of metals on the accuracy of the DGT technique. Analytical Chemistry.

Garcia-Ruiz, R., Lucena, J., Neill, F.X., 1999. Do bacteria regenerate phosphorus while decomposing seston? Marine and Freshwater Research, 50, 459-466.

Gimpel, J., Zhang, H., Hutchinson, W., Davison, W., 2001. Effect of solution composition, flow and deployment time on the measurement of trace metals by the diffusive gradient in thin films technique. Analytica Chimica Acta, 448, 93-103.

Glud, R.N., Gundersen, J.K., Jørgensen, B.B., Revsbech, N.P., Schulz, H.D., 1994. Diffusive and total oxygen-uptake of deep-sea sediments in the eastern south-Atlantic Ocean - in-situ and laboratory measurements. Deep-Sea Research Part I, 41, 1767-1788.

Glud, R.N., Gundersen, J.K., Revsbech, N.P., Jørgensen, B.B., 1994. Effects on the benthic diffusive boundary-layer imposed by microelectrodes. Limnology and Oceanography, 39, 462-467.

Glud, R.N., Jensen, K., Revsbech, N.P., 1995. Diffusivity in surficial sediments and benthic mats determined by use of a combined N_2O-O_2 microsensor. Geochimica et Cosmochimica Acta, 59, 231-237.

Glud, R.N., Ramsing, N.B., Gundersen, J.K., Klimant, I., 1996. Planar optrodes: A new tool for fine scale measurements of two-dimensional O_2 distribution in benthic communities. Marine Ecology Progress Series, 140, 217-226.

Glud, R.N., Gundersen, J.K., Holby, O., 1999. Benthic in-situ respiration in the upwelling area off central Chile. Marine Ecology-Progress Series, 186, 9-18.

Glud, R.N., Klimant, I., Holst, G., Kohls, O., Meyer, V., Kühl, M., Gundersen, J.K., 1999. Adaptation, test and in situ measurements with O2 microopt(r)odes on benthic landers. Deep-Sea Research Part I, 46, 171-183.

Glud, R.N., Tengberg, A., Kühl, M., Hall, P.O.J., Klimant, I., Host, G., 2001. An in situ instrument for planar O_2 optode measurements at benthic interfaces. Limnology and Oceanography, 46, 2073-2080.

Glud, R.N., Wenzhöfer, F., Tengberg, A., Middelboe, M., Oguri, K., Kitazato, H., 2005. Distribution of oxygen in surface sediments from central Sagami Bay, Japan: In situ measurements by microelectrodes and planar optodes. Deep-Sea Research Part I, 52, 1974-1987.

Glud, R.N., Berg, P., Fossing, H., Jørgensen, B.B., 2007. Effect of the diffusive boundary layer on benthic mineralization and O_2 distribution: A theoretical model analysis. Limnology and Oceanography, 52, 547-557.

Grundmanis, V., Murray, J.W., 1977. Nitrification and denitrification in marine sediments from Puget Sound. Limnology and Oceanography, 22, 804-813.

Hamblin, W.K., 1962. X-radiography in the study of structures in homogeneous sediments. Journal of Sedimentary Petrology, 32, 201-210.

Hamilton-Taylor, J., Smith, E., Davison, W., Sugiyama, M., 2005. Resolving and modeling the effects of Fe and Mn redox cycling on trace metal behavior in a seasonally anoxic lake. Geochimica et Cosmochimica Acta, 69, 1947–1960.

Hamner, W.M., Madin, L.P., Alldrege, A.L., Gilmer, R.W., Hamner, P.P., 1975. Underwater observations of gelatinous zooplankton: sampling problems, feeding biology, and behavior. Limnology and Oceanography, 20, 907-917.

Hanrahan, G., Patil, D.G., Wang, J., 2004. Electrochemical sensors for environmental monitoring: design, development and applications. Journal of Environmental Monitoring, 6, 657-664.

Harita, Y., Hori, T., Sugiyama, M., 2005. Release of trace oxyanions from littoral sediments and suspended particles induced by pH increase in the epilimnion of lakes. Limnology and Oceanography, 50, 636-645.

Harper, M.P., Davison, W., Tych, W., 1997. Temporal, spatial, and resolution constraints for in situ sampling devices using diffusional equilibration: dialysis and DET. Environmental Science and Technology, 31, 3110-3119.

Harper, M.P., Davison, W., Zhang, H., Tych, W., 1998. Kinetics of metal exchange between solids and solutions in sediments and soils interpreted from DGT measured fluxes. Geochimica et Cosmochimica Acta, 62, 2757–2770.

Harper, M.P., Davison, W., Tych, W., 1999. Estimation of pore water concentrations from DGT profiles: a modelling approach. Aquatic Geochemistry, 5, 337-355.

Harper, M.P., Davison, W., Tych, W., 1999. One-dimensional views of three-dimensional sediments. Environmental Science and Technology, 33, 2611-2616.

Harper, M.P., Davison, W., Tych, W., 2000. DIFS - a modelling and simulation tool for DGT induced trace metal remobilisation in sediments and soils. Environmental Modelling and Software, 15, 55-66.

Hartmann, P., Ziegler, W., Holst, G., Lübbers, D.W., 1997. Oxygen flux fluorescence lifetime imaging. Sensors and Actuators B, 38-39, 110-115.

Heezen, B.C., Hollister, C.D., 1971. The Face of the Deep. Oxford University Press, New York, pp. 659.

Heggie, D., Lewis, T., 1984. Cobalt in pore waters of marine sediments. Nature, 311, 453–455.

Helz, G.R., Vorlicek, T.P., Kahn, M.D., 2004. Molybdenum scavenging by iron monosulfide. Environmental Science and Technology, 38, 4263-4268.

Hessen, D.O., Agren, G.I., Anderson, T.R., Elser, J.J., de Reiter, P.C., 2004. Carbon sequestration in ecosystems: the role of stoichiometry. Ecology, 85, 1179-1192.

Hesslein, R.H., 1976. An in situ sampler for close interval pore water studies. Limnology and Oceanography, 21, 912-915.

Ho, T.-Y., Quigg, A., Finkel, Z.V., Milligan, A.J., Wyman, K., Falkowski, P.J., Morel, F.M.M., 2003. The elemental composition of some marine phytoplankton. Journal of Phycology, 39, 1145-1159.

Honeyman, B.D., Santschi, P.H., 1988. Metals in aquatic systems. Environmental Science and Technology, 22, 862-871.

Huerta-Diaz, M.A., Morse, J.W., 1990. A quantitative method for determination of trace metal concentrations in sedimentary pyrite. Marine Chemistry, 29, 119-144.

Huerta-Diaz, M.A., Morse, J.W., 1992. Pyritization of trace metals in anoxic sediments. Geochimica et Cosmochimica Acta, 56, 2681-2702.

Huerta-Diaz, M.A., Tessier, A., Carignan, R., 1998. Geochemistry of trace metals associated with reduced sulfur in freshwater sediments. Applied Geochemistry, 13, 213-233.

Hulth, S., Aller, R.C., Engström, P., Selander, E., 2002. A pH plate fluorosensor (optode) for early diagenetic studies of marine sediments. Limnology and Oceanography, 47, 212-220.

Hunter, K.S., Wang, Y.F., Van Cappellen, P., 1998. Kinetic modeling of microbially-driven redox chemistry of subsurface environments: coupling transport, microbial metabolism and geochemistry. Journal of Hydrology, 209, 53-80.

Iversen, N., Jørgensen, B.B., 1993. Diffusion coefficients of sulfate and methane in marine sediments: Influence of porosity. Geochimica et Cosmochimica Acta, 57, 571-578.

Jahnke, R., 1985. A model of microenvironments in deep-sea sediments: formation and effects on porewater profiles. Limnology and Oceanography, 30, 956-965.

Jensen, K., Revsbech, N.P., Nielsen, L.P., 1993. Microscale distribution of nitrification activity in sediment determined with a shielded microsensor for nitrate. Applied and Environmental Microbiology, 59, 3287-3296.

Jézéquel, D., Brayner, R., Metzger, E., Viollier, E., Prévot, F., Fiévet, F., 2007. Two-dimensional determination of dissolved iron and sulfur species in marine sediment pore-waters by thin-film based imaging. Thau lagoon (France). Estuarine Coastal and Shelf Science, 72, 420-431.

Johnson, R.G., 1974. Particulate matter at the sediment-water interface in coastal environments. Journal of Marine Research, 32, 313-330.

Jørgensen, B.B., 1977. Bacterial sulfate reduction within reduced microniches of oxidized marine-sediments. Marine Biology, 41, 7-17.

Jørgensen, B.B., 1978. A comparison of methods for the quantification of bacterial sulphate reduction in coastal marine sediments. III. Estimation from chemical and bacteriological field data. Geomicrobiology Journal, 1, 49-64.

Jørgensen, B.B., Glud, R.N., Holby, O., 2005. Oxygen distribution and bioirrigation in Arctic fjord sediments (Svalbard, Barents Sea). Marine Ecology Progress Series, 292, 85-95.

Klimant, I., Meyer, V., Kühl, M., 1995. Fiberoptic oxygen microsensors, a new tool in aquatic biology. Limnology and Oceanography, 40, 1159-1165.

König, B., Kohls, O., Holst, G., Glud, R.N., Kühl, M., 2005. Fabrication and test of sol-gel based planar oxygen optodes for use in aquatic sediments. Marine Chemistry, 97, 262-276.

Koretsky, C.M., Van Cappellen, P., DiChristina, T.J., Kostka, J.E., Lowe, K.L., Moore, C.M., Roychoudhury, A.N., Viollier, E., 2005. Salt marsh pore water geochemistry does not correlate with microbial community structure. Estuarine, Coastal and Shelf Science, 62, 233-251.

Koschorreck, M., Brookland, I., Matthias, A., 2003. Biogeochemistry of the sediment-water interface in the littoral of an acidic mining lake studied with microsensors and gel-probes. Journal of Experimental Marine Biology and Ecology, 285, 71-84.

Krantzberg, G., 1985. The influence of bioturbation on physical, chemical and biological parameters in aquatic environments: a review. Environmental Pollution (Series A), 39, 99-122.

Kristensen, E., Pilgaard, R., 2001. The role of fecal pellet deposition by leaf-eating sesarmid crabs on litter decomposition in a mangrove sediment (Phuket, Thailand). In: Aller, J.Y., Woodin, S.A., Aller, R.C., (Eds.), Organism-Sediment Interactions, University of South Carolina Press, Columbia, pp. 369-384.

Krom, M.D., Davison, P., Zhang, H., Davison, W., 1994. High-resolution pore-water sampling with a gel sampler. Limnology and Oceanography, 39, 1967-1972.

Kühl, M., 2005. Optical microsensors for analysis of microbial communities. Microsensors in Microbial Ecology, 397, 166-199.

Kühl, M., Revsbech, N.P., 2001. Biogeochemical microsensors for boundary layer studies. In: Boudreau, B.P., Jørgensen, B.B., (Eds.), The Benthic Boundary Layer: Transport Processes and Biogeochemistry, Oxford University Press, Oxford, pp. 404.

Kühl, M., Steuckart, C., Eickert, G., Jeroschewski, P., 1998. A H_2S microsensor for profiling biofilm and sediments: application in an acidic lake sediment. Aquatic Microbial Ecology, 15, 201-209.

Lasaga, A.C., The kinetic treatment of geochemical cycles, Geochimica et Cosmochimica Acta, 1980, 44, 815-828.

Lee, B.-G., Fisher, N.S., 1992. Decomposition and release of elements from zooplankton debris. Marine Ecology Progress Series, 88, 117-128.

Leermakers, M., Gao, Y., Gabelle, C., Lojen, S., Ouddane, B., Wartel, M., Baeyens, W., 2005. Determination of high resolution pore water profiles of trace metals in sediments of the Rupel River (Belgium) using DET (diffusive equilibration in thin films) and DGT (diffusive gradients in thin films) techniques. Water Air and Soil Pollution, 166, 265-286.

Lewandowski, J., Rüter, K., Hupfer, M., 2002. Two-dimensional small-scale variability of pore water phosphate in freshwater lakes: Results from a novel dialysis sampler. Environmental Science and Technology, 36, 2039-2047.

Lewandowski, J., Laskov, C., Hupfer, M., 2007. The relationship between *Chironomus plumosus* burrows and the spatial distribution of pore-water phosphate, iron and ammonium in lake sediments. Freshwater Biology, 52, 331-343.

Li, Y.H., Gregory, S., 1974. Diffusion of ions in sea water and deep sea sediments. Geochimica et Cosmochimica Acta, 38,703-714.

Liebsch, G., Klimant, I., Krause, C., Wolfbeis, O.S., 2001. Fluorescent imaging of pH with optical sensors using time domain dual lifetime referencing. Analytical Chemistry, 73, 4354-4363.

Lienemann, C.-P., Taillefert, M., Perret, D., Gaillard, J.-F., 1997. Association of cobalt and manganese in aquatic systems: chemical and microscopic evidence. Geochimica et Cosmochimica Acta, 61, 1437–1446.

Lovely, D.R., 1993. Dissimilatory metal reduction. Annual Review of Microbiology, 47, 263-290.

Luther, G.W., Brendel, P.J., Lewis, B.L., Sundby, B., Lefrancois, L., Silverberg, N., Nuzzio, D.B., 1998. Simultaneous measurement of O_2, Mn, Fe, I⁻, and S(-II) in marine pore waters with a solid-state voltammetric microelectrode. Limnology and Oceanography, 43, 325-333.

Luther, G.W., Reimers, C.E., Nuzzio, D.B., Lovalvo, D., 1999. In situ deployment of voltammetric, potentiometric, and amperometric microelectrodes from a ROV to determine dissolved O_2, Mn, Fe, S(-2), and pH in porewaters. Environmental Science and Technology, 33, 4352-4356.

M'Intosh, W.C., 1894. On certain homes or tubes formed by Annelids. The Annals and Magazine of Natural History Series 6, 1-18.

Martin, J.H., Knauer, G. A., 1973. The elemental composition of plankton. Geochimica et Cosmochimica Acta, 37, 1639-1653.

Martin, J.H., Bruland, K.W., Broenkow, W.W., 1976. Cadmium transport in the California Current. In: Windom, H.L., Duce, R.A., [eds.], Marine pollutant transfer, Lexington Books, Lexington, pp. 159-184.

McGee-Russell, S.M., Debruijn, W.C., Gosztonyi, G., 1990. Hot knife microtomy for large area sectioning and combined light and electron-microscopy in neuroanatomy and neuropathology. Journal of Neurocytology, 19, 655-661.

Meile, C., Tuncay, K., 2006. Scale dependence of reaction rates in porous media. Advances in Water Research, 29, 62-71.

Meile, C., Tuncay, K., Van Cappellen, P., 2003. Explicit representation of spatial heterogeneity in reactive transport models: application to bioirrigated sediments, Journal of Geochemical Exploration, 78-89, 231-234.

Mendham, J., Denney, R.C., Barnes, J.D., Thomas, M.J.K., 2000. Vogel's textbook of Quantitative Chemical Analysis (Sixth Edition), Prentice Hall, Harlow, pp. 806.

Mermillod-Blondin, F., Marie, S., Desrosiers, G., Long, B., de Montery, L., Michaud, E., Stora, G., 2003. Assessment of the spatial variability of intertidal benthic communities by axial tomodensitometry: importance of fine-scale heterogeneity. Journal of Experimental Marine Biology and Ecology, 287, 193-208.

Meyer, R.L., Kjaer, T., Revsbech, N.P., 2001. Use of NO_x^- microsensors to estimate the activity of sediment nitrification and NO_x^- consumption along an estuarine salinity, nitrate, and light gradient. Aquatic Microbial Ecology, 26, 181-193.

Meysman, F.J.R., Galaktionov, O.S., Cook, P.M.L., Janssen, F., Huettel, M., Middleberg, J.J., 2007. Quantifying biologically and physically induced flow and tracer dynamics in permeable sediments. Biogeosciences, 4, 627-646.

Michaud, E., Desrosiers, G., Long, B., de Montery, L., Crémer, J.-F., Pelletier, E., Locat, J., Gilbert, F., Stora, G., 2003. Use of axial tomography to follow temporal changes of benthic communities in an unstable sedimentary environment (Baie des Ha! Ha!, Saguenay Fjord). Journal of Experimental Marine Biology and Ecology, 285-286, 265-282.

Michel, P., Boutier, B., Herbland, A., Averty, B., Artigas, L.F., Auger, D., Chartier, E., 1998. Behaviour of arsenic on the continental shelf off the Gironde estuary: role of phytoplankton in vertical fluxes during spring bloom conditions. Oceanologica Acta, 21, 325-333.

Middelburg, J.J., 1989. A simple rate model for organic matter decomposition in marine sediments. Geochimica et Cosmochimica Acta, 53, 1577-1581.

Middelburg, J.J., Hoede, D., van der Sloot, H.A., van der Weijden, C.H., Wijkstra, J., 1988. Arsenic, antimony and vanadium in the North Atlantic Ocean. Geochimica et Cosmochimica Acta, 52, 2871-2878.

Millero, F.J., Schreiber, D.R., 1982. Use of the ion pairing model to estimate activity coefficients of the ionic components of natural waters. American Journal of Science, 282, 1508-1540.

Morford, J., Kalnejais, L., Martin, W., Francois, R., Karle, I.-M., 2003. Sampling marine pore waters for Mn, Fe, U, Re and Mo: modifications on diffusional equilibration thin film gel probes. Journal of Experimental Marine Biology and Ecology, 285-286, 85-103.

Morford, J.L., Emerson, S.R., Breckel, E.J., Kim, S.H., 2005. Diagenesis of oxyanions (V, U, Re and Mo) in pore waters and sediments from a continental margin, Geochimica et Cosmochimica Acta, 69, 5021-5032.

Morse, J.W., Luther, G.W., 1999. Chemical influences on trace metal-sulphide interactions in anoxic sediments. Geochimica et Cosmochimica Acta, 63, 3373-3378.

Morse, J.W., Eldridge, P.M., 2007. A non-steady state diagenetic model for changes in sediment biogeochemistry in response to seasonally hypoxic/anoxic conditions in the "dead zone" of the Louisiana shelf. Marine Chemistry, 106, 239-255.

Morse, J.W., DiMarco, S.F., Herbert, A.B., Sell, K.S., 2003. A scaling approach to spatial variability in early diagenetic processes. Hydrobiologia, 494, 25-29.

Mortimer, R.J.G., Krom, M.D., Hall, P.O.J., Hulth, S., Stahl, H., 1998. Use of gel probes for the determination of high resolution solute distributions in marine and estuarine pore waters. Marine Chemistry, 63, 119-129.

Mortimer, R.J.G., Krom, M.D., Harris, S.J., Hayes, P.J., Davies, I.M., Davison, W., Zhang, H., 2002. Evidence for suboxic nitrification in recent marine sediments. Marine Ecology Progress Series, 236, 31-35.

Motelica-Heino, M., Davison, W., 2003. Trace metals dynamics in surface sediments investigated by DGT micro-scale measurements. Journal de Physique IV, 107, 899-902.

Motelica-Heino, M., Naylor, C., Zhang, H., Davison, W., 2003. Simultaneous release of metals and sulfide in lacustrine sediment. Environmental Science and Technology, 37, 4374-4381.

Müller, B., Stierli, R., 1999. In situ determination of sulfide profiles in sediment porewaters with a miniaturized Ag/Ag_2S electrode. Analytica Chimica Acta, 401, 257-264.

Murray, J.W., Emerson, S., Jahnke, R., 1980. Carbonate saturation and the effect of pressure on the alkalinity of interstitial waters from the Guatemala Basin. Geochimica et Cosmochimica Acta, 44, 963-972.

Naylor, C., Davison, W., Motelica-Heino, M., Van Den Berg, G., Van Der Heijdt, L., 2004. Simultaneous release of sulfide with Fe, Mn, Ni and Zn in marine harbour sediment measured using a combined metal/sulfide DGT probe. Science of the Total Environment, 328, 275–286.

Naylor, C., Davison, W., Motelica-Heino, M., van den Berg, G.A., van der Heijdt, L.M., 2006. Potential kinetic availability of metals in sulphidic freshwater sediments. Science of the Total Environment, 357, 208-220.

Nicholas, D.R., Ramamoorthy, S., Palace, V., Spring, S., Moore, J.N., Rosenzweig, R.F., 2003. Biological transformations of arsenic in circumneutral freshwater sediments. Biodegradation, 14, 123-137.

Oguri, K., Kitazato, H., Glud, R.N., 2006. Platinum octaetylporphyrin based planar optodes combined with an UV-LED excitation light source: An ideal tool for high-resolution O_2 imaging in O_2 depleted environments. Marine Chemistry, 100, 95-107.

Otero, X.L., Macias, F., 2003. Spatial variation in pyritization of trace metals in salt-marsh soils. Biogeochemistry, 62, 59-86.

Pamatmat, M.M., Fenton, D., 1968. An instrument for measuring subtidal benthic metabolism in situ. Limnology and Oceanography, 13, 537-540.

Papaspyrou, S., Gregersen, T., Kristensen, E., Christensen, B., Cox, R.P., 2006. Microbial reaction rates and bacterial communities in sediment surrounding burrows of two nereidid polychaetes (*Nereis diversicolor* and *N. virens*). Marine Biology, 148, 541-550.

Perez, K.T., Davey, E.W., Moore, R.H., Bunn, P.R., Rosol, M.S., Cardin, J.A., Johnson, R.L., Kopans, D.N., 1999. Application of computer-aided tomography (CT) to the study of estuarine benthic communities. Ecological Applications, 9, 1050-1058.

Petersen, W., Wallmann, K., Pinglin, L., Schroeder, F., Knauth, H.-D., 1995. Exchange of trace elements at the sediment-water interface during early diagenesis processes. Marine and Freshwater Research, 46, 19–26.

Pike, J., Bernhard, J.M., Moreton, S.G., Butler, I.B., 2001. Microbioirrigation of marine sediments in dysoxic environments: implications for early sediment fabric formation and diagenetic processes. Geology, 29, 923-926.

Ploug, H., Kühl, M., Buchholz-Cleven, B., Jørgensen, B.B., 1997. Anoxic aggregates - an ephemeral phenomenon in the pelagic environment? Aquatic Microbial Ecology, 13, 285-294.

Polerecky, L., Volkenborn, N., Stief, P., 2006. High temporal resolution oxygen imaging in bioirrigated sediments. Environmental Science and Technology, 40, 5763-5769.

Raiswell, R., 1993. Kinetic controls on depth variations in localised pyrite formation. Chemical Geology, 107, 467-469.

Raiswell, R., Whaler, K., Dean, S., Coleman, M.L., Briggs, D.E.G., 1993. A simple three-dimensional model of diffusion-with-precipitation applied to localised pyrite formation in framboids, fossils and detrital iron minerals. Marine Geology, 113, 89-100.

Raiswell, R., Newton, R., Bottrell, S.H., Coburn, P.M., Briggs, D.E.G., Bond, D.P.G., Poulton, S.W., 2008. Turbidite depositional influences on the diagenesis of Beecher's Trilobite Bed and the Hunsrück Slate; sites of soft tissue pyritization. American Journal of Science, 308, 105-129.

Reimers, C.E., 1987. An in situ microprofiling instrument for measuring interfacial pore water gradients: methods and oxygen profiles from the north Pacific-Ocean. Deep-Sea Research Part A, 34, 2019-2035.

Reimers, C.E., 2007. Applications of microelectrodes to problems in chemical oceanography. Chemical Reviews, 107, 590-600.

Reimers, C.E., Fischer, K.M., Merewether, R., Smith, K.L., Jahnke, R.A., 1986. Oxygen microprofiles measured insitu in deep ocean sediments. Nature, 320, 741-744.

Ren, J., Packman, A.I., 2004. Modelling of Simultaneous Exchange of Colloids and Sorbing contaminants between streams and streambeds. Environmental Science and Technology, 38, 2901-2911.

Ren, J., Packman, A.I., 2004. Stream-Subsurface exchange of zinc in the presence of silica and kaolinite colloids. Environmental Science and Technology, 38, 6571-6581.

Ren, J., Packman, A.I., 2005. Coupled stream-subsurface exchange of colloidal hematite and dissolved zinc, copper, and phosphate. Environmental Science and Technology, 39, 6387-6394.

Revsbech, N.P., 1989. An oxygen microsensor with a guard cathode. Limnology and Oceanography, 34, 474-478.

Revsbech, N.P., 2005. Analysis of microbial communities with electrochemical microsensors and microscale biosensors. Microsensors in Microbial Ecology, 397, 147-166.

Revsbech, N.P., Ward, D.M., 1983. Oxygen microelectrode that is insensitive to medium chemical-composition - use in an acid microbial mat dominated by *Cyanidium-caldarium*. Applied and Environmental Microbiology, 5, 755-759.

Revsbech, N.P., Jørgensen, B.B., Blackburn, T.H., 1980. Oxygen in the sea bottom measured with a microelectrode. Science, 207, 1355-1356.

Revsbech, N.P., Sorensen, J., Blackburn, T.H., Lomholt, J.P., 1980. Distribution of oxygen in marine-sediments measured with microelectrodes. Limnology and Oceanography, 25, 403-411.

Revsbech, N.P., Madsen, B., Jørgensen, B.B., 1986. Oxygen production and consumption in sediments determined at high spatial-resolution by computer-simulation of oxygen microelectrode data. Limnology and Oceanography, 31, 293-304.

Rhoads, D.C., Young, D.K., 1970. The influence of deposit-feeding organisms on sediment stability and community trophic structure. Journal of Marine Research, 28,150-178.

Rhoads, D.C., Cande, S., 1971. Sediment profile camera for in situ study of organism-sediment relations. Limnology and Oceanography, 16, 110-114.

Rhoads, D.C., Boyer, L.F., 1982. The effects of marine benthos on physical properties of sediments: a successional perspective. In: McCall, P.L., Tevesz, M.J.S., (Eds.), Animal-Sediment Relations, Plenum Press, New York, pp 3-52.

Robson, R.L., Eady, R.R., Richardson, T.H., Miller, R.W., Hawkins, M., Postgate, J.R., 1986. The alternative nitrogenase of *Azotobacter chroococcum* is a vanadium enzyme. Nature, 322, 388-390.

Rogers, N.J., Apte, S.C., 2003. Azo dye method for mapping relative sediment enzyme activity in situ at precise spatial locations. Environmental Science and Technology, 38, 5134-5140.

Rosenberg, R., Davey, E., Gunnarsson, J., Norling, K., Frank, F., 2007. Application of computer-aided tomography to visualize and quantify biogenic structures in marine sediments. Marine Ecology Progress Series, 331, 23-34.

Roulier, J.L., Tusseau-Vuillemin, M.H., Coquery, M., Geffard, O., Garric, J., 2008. Measurement of dynamic mobilization of trace metals in sediments using DGT and comparison with bioaccumulation in *Chironomus riparius*: First results of an experimental study. Chemosphere, 70, 925-932.

Rowe, G.T., Boland, G.S., Briones, E.G.E., Cruz-Kaegi, M.E., Newton, A., Piepenberg, D., Walsh, I., Deming, J., 1997. Sediment community biomass and respiration in the Northeast Water Polynya, Greenland: a numerical simulation of benthic lander and spade core data. Journal of Marine Systems, 10, 497-515.

Rysgaard, S., Thamdrup, B., Risgaard-Petersen, N., Fossing, H., Berg, P., Christensen, P.B., Dalsgaard, T., 1998. Seasonal carbon and nitrogen mineralization in a high-Arctic coastal marine sediment, Young Sound, Northeast Greenland. Marine Ecology Progress Series, 179, 262-276.

Sagemann, J., Bale, S.J., Briggs, D.E.G., Parkes, R.J., 1999. Controls on the formation of authigenic minerals in association with decaying organic matter: an experimental approach. Geochimica et Cosmochimica Acta, 63, 1083-1095.

Scally, S., Davison, W., Zhang, H., 2006. Diffusion coefficients of metals and metal complexes in hydrogels used in diffusive gradients in thin films. Analytica Chimica Acta, 558, 222-229.

Schaffner, L.C., Dellapenna, T.M., Hinchey, E.K., Friedrichs, C.T., Neubauer, M.T., Smith M.E., Kuehl, S.A., 2001. Physical energy regimes, seabed dynamics, and organism-sediment interactions along an estuarine gradient. In: Aller, J.Y., Woodin, S.A., Aller, R.C., (Eds.), Organism-Sediment Interactions, University of South Carolina Press, Columbia, pp. 159-179.

Schroeder, C.R., Neurauter, G., Klimant, I., 2007. Luminescent dual sensor for time-resolved imaging of pCO$_2$ and pO$_2$ in aquatic systems. Microchimica Acta, 158, 205-218.

Schwertmann, U., Cornell, R.M., 2000. Iron Oxides in the Laboratory, Preparation and Characterization, Second Edition. Wiley-VCH, Weinheim, pp 188.

Sell, K.S., Morse, J.W., 2006. Dissolved Fe^{2+} and $\sum H_2S$ behavior in sediments seasonally overlain by hypoxic-to-anoxic waters as determined by CSV microelectrodes. Aquatic Geochemistry, 12, 179–198.

Senior, E., Lindström, E.B., Banat, I.M., Nedwell, D.B., 1982. Sulfate reduction and methanogenesis in the sediment of a saltmarsh on the east coast of the United Kingdom. Applied Environmental Microbiology, 43, 987-996.

Shanks, A.L., Reeder, M.L., 1993. Reducing microzones and sulphide production in marine snow. Marine Ecology Progress Series, 96, 43-47.

Shaw, T.J., Gieskes, J.M., Jahnke, R.A., 1990. Early diagenesis in differing depositional-environments - the response of transition-metals in pore water. Geochimica et Cosmochimica Acta, 54, 1233-1246.

Shiller, A.M., Boyle, E.A.,1987. Dissolved vanadium in rivers and estuaries. Earth and Planetary Science Letters, 86, 214-224.

Shiller, A.M., Mao, L., 1999. Dissolved vanadium on the Louisiana Shelf: effect of oxygen depletion. Continental Shelf Research, 19, 1007-1020.

Shuttleworth, S., 1999. Heavy metal geochemistry in lakes: temporal and spatial variations measured with DET and DET. Ph.D. thesis, Lancaster University, UK.

Shuttleworth, S.M., Davison, W., Hamilton-Taylor, J., 1999. Two-dimensional and fine structure in the concentrations of iron and manganese in sediment pore-waters. Environmental Science and Technology, 33, 4169-4175.

Skogerboe, R.K., Wilson, S.A., 1981. Reduction of ionic species by fulvic acid. Analytical Chemistry, 53, 228-232.

Sochaczewski, L., Tych, W., Davison, B., Zhang, H., 2007. 2D DGT induced fluxes in sediments and soils (2D DIFS). Environmental Modelling and Software, 22, 14-23.

Sochaczewski, Ł., Stockdale, A., Davison, W., Tych, W., Zhang, H., 2008. A three-dimensional reactive transport model for sediments, incorporating microniches. Environmental Chemistry, 5, 218-225.

Stahl, H., Glud, A., Schröder, C.R., Klimant, I., Tengberg, A., Glud, R.N., 2006. Time-resolved pH imaging in marine sediments with a luminescent planar optode. Limnology and Oceanography – Methods, 4, 336-345.

Stief, P., Nazarova, L., de Beer, D., 2005. Chimney construction by *Chironomus riparius* larvae in response to hypoxia: microbial implications for

freshwater sediments. Journal of the North American Benthological Society, 24, 858-871.

Stockdale, A., Davison, W., Zhang, H., 2008. High-resolution two-dimensional quantitative analysis of phosphorus, vanadium and arsenic, and qualitative analysis of sulfide, in a freshwater sediment, Environmental Chemistry, 5, 143-149.

Stockdale, A., Davison, W., Zhang, H., revisions submitted. Micro-scale biogeochemical heterogeneity in sediments: A review of available techniques and observed evidence. Earth-Science Reviews.

Stockdale, A., Davison, W., Zhang, H., submitted manuscript. Sulphide evolution from faecal pellets and other microniches within sub oxic surface sediment: The effects on the geochemistry of iron and trace elements. Geochimica et Cosmochimica Acta.

Strang, W.G., Fix, G.J., 1973. An Analysis of the Finite Element Method, Prentice-Hall, New Jersey, pp 306.

Strömberg, N., Hulth, S., 2005. Assessing an imaging ammonium sensor using time correlated pixel-by-pixel calibration. Analytica Chimica Acta, 550, 61-68.

Sukola, K., Wang, F., Tessier, A., 2005. Metal-sulfide species in oxic waters. Analytica Chimica Acta, 528, 183-195.

Sweerts, J.-P.R.A., St Louis, V., Cappenberg, T.E., 1989. Oxygen concentration profiles and exchange in sediment cores with circulated overlying water. Freshwater Biology, 21, 401-409.

Taghon G.L., Nowell, A.R.M., Jumars, P.A., 1984. Transport and breakdown of fecal pellets: biological and sedimentological consequences. Limnology and Oceanography, 29, 64-72.

Taillefert, M., Luther, G.W., Nuzzio, D.B., 2000. The application of electrochemical tools for in situ measurements in aquatic systems. Electroanalysis, 12, 401-412.

Taillefert, M., Macgregor, B., Galliard, J.-F., Lienemann, C.-P., Perret, D., Stahl, D., 2002. Evidence for a dynamic cycle between Mn and Co in the water column of a stratified lake. Environmental Science and Technology, 36, 468–476.

Taillefert, M., Neuhuber, S., Bristow, G., 2007. The effect of tidal forcing on biogeochemical processes in intertidal salt marsh sediments. Geochemical Transactions, 8:6.

Tankere-Muller, S., Zhang, H., Davison, W., Finke, N., Larsen, O., Stahl, H., Glud, R.N., 2007. Fine scale remobilisation of Fe, Mn, Co, Ni, Cu and Cd in contaminated marine sediment. Marine Chemistry, 106, 192-207.

Teasdale, P.R., Hayward, S., Davison, W., 1999. In situ, high-resolution measurement of dissolved sulfide using diffusive gradients in thin films with computer-imaging densitometry. Analytical Chemistry, 71, 2186-2191.

Tessier, A., Fortin, D., Belzile, N., DeVitre, R.R., Leppard, G.G., 1996. Metal sorption to diagenetic iron and manganese oxyhydroxides and associated organic matter: narrowing the gap between field and laboratory measurements. Geochimica et Cosmochimica Acta, 60, 387-404.

Tezuka, Y., 1990. Bacterial regeneration of ammonium and phosphate as affected by the carbon : nitrogen : phosphorus ratio of organic substrates. Microbial Ecology, 19, 227-238.

Touzani, R., 2003. OFELI (Object Finite Element LIbrary). Université Blaise Pascal, Clermont Ferrand. Available at www.ofeli.net, accessed January 2007.

Tribovillard, N., Alego, T.J., Lyons, T., Riboulleau, A., 2006. Trace metals as paleoredox and paleoproductivity proxies: An update. Chemical Geology, 232, 12-32.

Trouwborst, R.E., Johnston, A., Koch, G., Luther G.W., Pierson B.K., 2007. Biogeochemistry of Fe(II) oxidation in a photosynthetic microbial mat: Implications for Precambrian Fe(II) oxidation. Geochimica et Cosmochimica Acta, 71, 4629-4643.

Tsygankov, A.A., 2007. Nitrogen-fixing cyanobacteria: A review. Applied Biochemistry and Microbiology, 43, 250-259.

Uehlinger, U., 1986. Bacteria and phosphorus regeneration in lakes. An experimental study. Hydrobiologia, 135, 197-206.

Van Cappellen, P., Galliard, J.-F., Rabouille, C., 1993. Biogeochemical transformations in sediments: kinetic models of early diagenesis. In Woolast, R., Mackenzie, F.T., Chou, L., (Eds.), Interactions of C, N, P and S Biogeochemical Cycles and Global Change. Springer-Verlag, Berlin, pp. 401-445.

Van Cappellen, P., Wang, Y.F., 1996. Cycling of iron and manganese in surface sediments: a general theory for the coupled transport and reaction of carbon, oxygen, nitrogen, sulfur, iron, and manganese. American Journal of Science, 296, 197-243.

Viollier, E., Rabouille, C., Apitz, S.E., Breuer, E., Chaillou, G., Dedieu, K., Furukawa, Y., Grenz, C., Hall, P., Janssen, F., Morford, J.L., Poggiale, J.C., Roberts,

S., Shimmield, T., Taillefert, M., Tengberg, A., Wenzhöfer, F., Witte, U., 2003. Benthic biogeochemistry: state of the art technologies and guidelines for the future of in situ survey. Journal of Experimental Marine Biology and Ecology, 285, 5-31.

Wallschläger, D., Stadey, C.J., 2007. Determination of (oxy)thioarsenates in sulfidic waters. Analytical Chemical, 79, 3873-3880.

Wang Y., van Cappellen, P., 1996. A multicomponent reactive transport model of early diagenesis: Application to redox cycling in coastal marine sediments. Geochimica et Cosmochimica Acta, 60, 2993-3014.

Wang, F.Y., Tessier, A., Hare, L., 2001. Oxygen measurements in the burrows of freshwater insects. Freshwater Biology, 46, 317-327.

Wanty, R.B., Goldhaber, M.B., 1992. Thermodynamics and kinetics of reactions involving vanadium in natural systems: Accumulation of vanadium in sedimentary rocks. Geochimica et Cosmochimica Acta, 56, 1471-1483.

Warnken, K.W., Zhang, H., Davison, W., 2004. Analysis of polyacrylamide gels for trace metals using diffusive gradients in thin films and laser ablation inductively coupled plasma mass spectrometry. Analytical Chemistry, 76, 6077-6084.

Warnken, K.W., Zhang, H., Davison, W., 2004. Performance characteristics of suspended particulate reagent-iminodiacetate as a binding agent for diffusive gradients in thin films. Analytica Chimica Acta, 508, 41-51.

Warnken, K.W., Zhang, H., Davison, W., 2007. In situ monitoring and dynamic speciation measurements in solution using DGT. In: Greenwood, R., Mills, G., Vrana, B., (Eds.), Comprehensive Analytical Chemistry, Volume 48, Passive Sampling Techniques in Environmental Monitoring, Elsevier, pp. 251-278.

Watling, L., 1988. Small-scale features of marine sediments and their importance to the study of deposit-feeding. Marine Ecology-Progress Series, 47, 135-144.

Watson, A.T., 1890. The tube building habits of *Terebella littoralis*. Journal of the Royal Microscopical Society, 10, 685-689.

Wenzhöfer, F., Glud, R.N., 2004. Small-scale spatial and temporal variability in coastal benthic O_2 dynamics: effects of fauna activity. Limnology and Oceanography, 49, 1471-1481.

Wenzhöfer, F., Adler, M., Kohls, O., Hensen, C., Strotmann, B., Boehme, S., Schulz, H.D., 2001. Calcite dissolution driven by benthic mineralization in the deep-

sea: in situ measurements of Ca^{2+}, pH, pCO_2 and O_2. Geochimica et Cosmochimica Acta, 65, 2677-2690.

Wenzhöfer, F., Holby, O., Kohls, O., 2001. Deep penetrating benthic oxygen profiles measured in situ by oxygen optodes. Deep-Sea Research Part I, 48, 1741-1755.

Westrich, J.T., Berner, R.A., 1984. The role of sedimentary organic-matter in bacterial sulfate reduction - the G model tested. Limnology and Oceanography, 29, 236-249.

Widerlund, A., Davison, W., 2007. Size and density distribution of sulfide-producing microniches in lake sediments. Environmental Science and Technology, 41, 8044-8049.

Wijsman, J.W.M., Herman, P.M.J., Middelburg, J.J., Soetaert, K., 2002. A model for early diagenetic processes in sediments of the continental shelf of the Black Sea. Estuarine Coastal and Shelf Science, 54, 403-421.

Yeh, G.T., Tripathi, V.S., 1989. A critical evaluation of recent developments in hydrogeochemical transport models of reactive multichemical components. Water Resources Research, 25, 93-108.

Yu, K.T., Lam, M.H.W., Yen, Y.F., Leung, A.P.K., 2000. Behavior of trace metals in the sediment pore waters of intertidal mudflats of a tropical wetland. Environmental Toxicology and Chemistry, 19, 535-542.

Zhang, H., Davison, W., Miller, S., Tych, W., 1995. In-situ high-resolution measurements of fluxes of Ni, Cu, Fe, and Mn and concentrations of Zn and Cd in porewaters by DGT. Geochimica et Cosmochimica Acta, 59, 4181-4192.

Zhang, H., Davison, W., Gadi, R., Kobayashi, T., 1998. In situ measurements of dissolved phosphorus in natural waters using DGT. Analytica Chimica Acta, 370, 29-38.

Zhang, H., Davison, W., Ottley, C., 1999. Remobilisation of major ions in freshly deposited lacustrine sediment at overturn. Aquatic Sciences, 61, 354-361.

Zhang, H., Davison, W., Mortimer, R.J.G., Krom, M.D., Hayes, P.J., Davies, I.M., 2002. Localised remobilization of metals in a marine sediment. Science of the Total Environment, 296, 175-187.

Zheng, Y., Anderson, R.F., van Gleen, A., Kuwabara, J., 2000. Authigenic molybdenum formation in marine sediments: a link to porewater sulphide in the Santa Barbara Basin. Geochimica et Cosmochimica Acta, 64, 4165-4178.

Zhu, Q.Z., Aller, R.C., Fan, Y.Z., 2005. High-performance planar pH fluorosensor for two-dimensional pH measurements in marine sediment and water. Environmental Science and Technology, 39, 8906-8911.

Zhu, Q.Z., Aller, R.C., Fan, Y.Z., 2006. A new ratiometric, planar fluorosensor for measuring high resolution, two-dimensional pCO_2 distributions in marine sediments. Marine Chemistry, 101, 40-53.

Zhu, Q.Z., Aller, R.C., Fan, Y.Z., 2006. Two-dimensional pH distributions and dynamics in bioturbated marine sediments. Geochimica et Cosmochimica Acta, 70, 4933-4949.

Appendix A

Description of characteristic response time in relation to DGT and the DIFS models, and the derivation of the related equations.

DGT (diffusive gradients in thin-films) has been used for the measurement of Fe, Mn and trace metals in both freshwater (Motelica-Heino et al, 2003) and marine sediments (Fones et al, 2004). DGT measured concentration is only representative of porewater concentration when there is sufficient resupply from the solid phase to replenish the depleted porewater. A more typical scenario during DGT deployment is that there is a partial resupply from the solid phase. In these situations DGT measurement is best treated as an assessment of the solute that can be supplied locally in response to a perturbation. Cases of insufficient resupply have been considered previously for sediment DGT analysis (Zhang et al, 2002).

The DIFS (DGT induced fluxes in sediments) models were developed to yield numerical solutions to these dynamic systems. Two models have been developed using one-dimensional (Harper et al, 2000) and two-dimensional (Sochaczewski et al, 2007) diffusion. The DIFS models use a single pool of trace metal linearly distributed between the aqueous and sorbed phases (with distribution coefficient K_d). The kinetics are accounted for by adsorption and desorption rate constants (k_f and k_b) with transport within the system controlled by diffusion. DIFS has been used to assess resupply in saturated soils (e.g. Ernstberger et al, 2002; 2005) and recent work has applied DIFS to contaminated freshwater reservoir sediments (Roulier et al, 2008).

Theory

For an equilibrium reaction of the form shown in Equation 1 the change in concentration of B over time can be expressed as a differential equation (Eq. 2).

$$[A]_{aq} \underset{k_b}{\overset{k_f}{\rightleftharpoons}} [B]_{sorb} \tag{3}$$

$$\frac{d[B]_t}{dt} = k_f[A]_t - k_b[B]_t \tag{4}$$

Solving this equation gives the following result.

$$[B]_t = \frac{k_f P}{(k_f + k_b)}(1 - e^{-(k_f+k_b)t}) + [B]_i e^{-(k_f+k_b)t} \tag{5}$$

Where P is the sum of the initial concentrations of A and B, $[B]_i$ represents the initial concentration of B and $[B]_t$ is the concentration of B after time, t. As the pool size (P) and the rate constants (k_f and k_b) are unchanged throughout the reaction, the equation can be simplified (Eq. 4).

$$[B]_t = x(1 - e^{-(k_f+k_b)t}) + [B]_i e^{-(k_f+k_b)t} \tag{6}$$

If at time zero, [B] is zero, the equation can be further simplified (Eq. 5).

$$[B]_t = x(1 - e^{-(k_f+k_b)t}) \tag{7}$$

As t approaches ∞, the exponential term approaches zero and [B] approaches equilibrium (i.e. the maximum value). When the sum of k_f and k_b equals the reciprocal of t (Eq. 6), the exponential term becomes e^{-1} and the concentration of B is 63% (1 − e^{-1}) of the equilibrium value.

$$k_f + k_b = t_c^{-1} \tag{8}$$

Thus, the relationship in Eq. 6 can be seen as a characteristic response time of the system to approach equilibrium. If $k_f \gg k_b$ then Eq. 6 simplifies to Eq. 7.

$$k_f = t_c^{-1} \tag{9}$$

The distribution coefficient K_d can be directly related to the partitioned concentrations and the sorption/desorption rate constants (Eq. 8). Where p_c is the particle concentration.

$$K_d = \frac{C_{sorbed}}{C_{solution}} = \frac{k_f}{k_b p_c} \qquad (10)$$

Combining Equations 7 and 8 gives the relationship between the characteristic response time, the desorption rate constant and the partition coefficient (Eq. 9).

$$t_c = \frac{1}{K_d k_b p_c} \qquad (11)$$

These relationships defined above allow the sorption/desorption rate constants to be calculated from the DIFS fitted t_c and K_d values.

Full step-wise derivations

Solving the equilibrium value of a zero order reaction of the form:

$$[A]_{aq} \underset{k_b}{\overset{k_f}{\rightleftharpoons}} [B]_{sorb} \qquad\qquad (A1)$$

Let: $_i$ represent the initial value

$_t$ represent the value at time t

P represent the concentration of the entire pool of A and B, i.e.

$$P = [A]_i + [B]_i \qquad\qquad (A2)$$

The changes in concentration of the components can be expressed as:

$$-\frac{d[A]}{dt} = \frac{d[B]}{dt} = k_f [A]_t - k_b [B]_t \qquad\qquad (A3)$$

The concentration of A at time t can be expressed as:

$$[A]_t = [B]_i - [B]_t + [A]_i \qquad\qquad (A4)$$

The concentration of A being proportional to the initial value of A minus any loss due to formation of B (i.e. initial B minus B at time t)

Substituting Equation A4 into A3 gives:

$$\frac{d[B]}{dt} = k_f ([B]_i - [B]_t + [A]_i) - k_b [B]_t \qquad\qquad (A5)$$

$$= k_f [B]_i - k_f [B]_t + k_f [A]_i - k_b [B]_t \qquad\qquad (A6)$$

rearranging A2 and substituting for $[A]_i$ gives:

$$= k_f [B]_i - k_f [B]_t + k_f (P - [B]_i) - k_b [B]_t \qquad\qquad (A7)$$

$$= k_f [B]_i - k_f [B]_t + k_f P - k_f [B]_i - k_b [B]_t \qquad\qquad (A8)$$

Which simplifies to:

$$= k_f P - (k_f + k_b)[B]_t \qquad\qquad (A9)$$

Multiplying the first expression by Equation A10:

$$\frac{(k_f + k_b)}{(k_f + k_b)}(=1) \tag{A10}$$

gives:

$$\frac{d[B]}{dt} = \frac{k_f P(k_f + k_b)}{(k_f + k_b)} - (k_f + k_b)[B]_t \tag{A11}$$

$$= (k_f + k_b)\left(\frac{k_f P}{(k_f + k_b)} - [B]_t\right) \tag{A12}$$

$$\frac{d[B]}{\frac{k_f P}{(k_f + k_b)} - [B]_t} = (k_f + k_b)dt \tag{A13}$$

Integration of:

$$\int_t^i \frac{d[B]}{\frac{k_f P}{(k_f + k_b)} - [B]_t} = (k_f + k_b)\int_t^0 dt \tag{A14}$$

Gives:

$$-\left[\ln\left(\frac{k_f P}{(k_f + k_b)} - [B]_t\right) - \ln\left(\frac{k_f P}{(k_f + k_b)} - [B]_i\right)\right] = (k_f + k_b)t \tag{A15}$$

$$-\left[\ln\frac{\left(\frac{k_f P}{(k_f + k_b)} - [B]_t\right)}{\left(\frac{k_f P}{(k_f + k_b)} - [B]_i\right)}\right] = (k_f + k_b)t \tag{A16}$$

$$\frac{\left(\frac{k_f P}{(k_f + k_b)} - [B]_t\right)}{\left(\frac{k_f P}{(k_f + k_b)} - [B]_i\right)} = e^{-(k_f + k_b)t} \tag{A17}$$

$$\frac{k_f P}{(k_f + k_b)} - [B]_t = \left(\frac{k_f P}{(k_f + k_b)} - [B]_i\right)e^{-(k_f + k_b)t} \tag{A18}$$

A5

$$\frac{k_f P}{(k_f + k_b)} - [B]_t = \frac{k_f P}{(k_f + k_b)} e^{-(k_f + k_b)t} - [B]_i e^{-(k_f + k_b)t} \tag{A19}$$

$$[B]_t = \frac{k_f P}{(k_f + k_b)} - \frac{k_f P}{(k_f + k_b)} e^{-(k_f + k_b)t} + [B]_i e^{-(k_f + k_b)t} \tag{A20}$$

Giving the final solution:

$$[B]_t = \frac{k_f P}{(k_f + k_b)}(1 - e^{-(k_f + k_b)t}) + [B]_i e^{-(k_f + k_b)t} \tag{A21}$$

As the total pool size and the rate constants are the same at any point in the reaction the expression containing these can be substituted for a constant:

$$[B]_t = x(1 - e^{-(k_f + k_b)t}) + [B]_i e^{-(k_f + k_b)t} \tag{A22}$$

Special cases

Case 1. $[B]_{t=0} = 0$

Equation A21 is simplified to:

$$[B]_t = x(1 - e^{-(k_f + k_b)t}) \tag{A23}$$

Case 2. $t \to \infty$

Allowing $t \to \infty$ gives the maximum (or equilibrium) value, as the exponential function tends towards zero. i.e. $[B] = x$

Case 3. $k_f + k_b = t^{-1}$

Using Equation A23

The exponential function becomes e^{-1} giving the equation:

$$[B]_t = x(1 - 0.37) = 0.63x \qquad\qquad (A24)$$

As x represents the equilibrium concentration the 63% equilibrium response time can be calculated from the reciprocal of the sum of the forward and reverse rate constants.

Using Equation A22

If the system is not starting from a zero concentration of B then the initial concentration must be considered. This equation allows the time required to reach intermediate levels of equilibrium recovery to be calculated. For example if a system was at 80% at $t = 0$ and 90% at t = y the elapsed time can be calculated. $k_f + k_b = t^{-1}$ can also be shown to be the 63% recovery between the two equilibrium values.

Appendix B

3D Sediment Model for Microniches (3D TREAD): A Practical User Guide

---

Contents:

---

1. What is 3D TREAD?

3D TREAD is a dynamic numerical diagenetic model for sediments, allowing specification of spherical zones with different geochemistry from the surrounding matrix (microniches). The flexible specification of components and reactions allows the user to define any required components. The full numerical framework and an example of the model application are described in the original paper presenting this model (Sochaczewski et al, 2008. Environmental Chemistry, 5, 218-225. (http://dx.doi.org/10.1017/EN08006)).

2. Requirements

3D TREAD is a 32 bit application designed to run on Windows XP and Vista systems. Required disk space will vary depending on model inputs, a minimum of 500 MB free disk space is recommended. 3D TREAD has no other specific hardware requirements. However, a fast processor (at least 1.5GHz) and a minimum of 1GB of RAM is

recommended. The MathWorks programme Matlab is required for extracting output data.

3. Installing and running 3D TREAD

All required files are included in a zip file (downloadable from http://www.es.lancs.ac.uk/wdgroup/index.htm). Once the files are extracted the model can be run directly using the executable file 'sediment3d.exe'. This executable opens the graphical user interface (GUI) main menu, shown in Figure 1, which controls the input parameters.
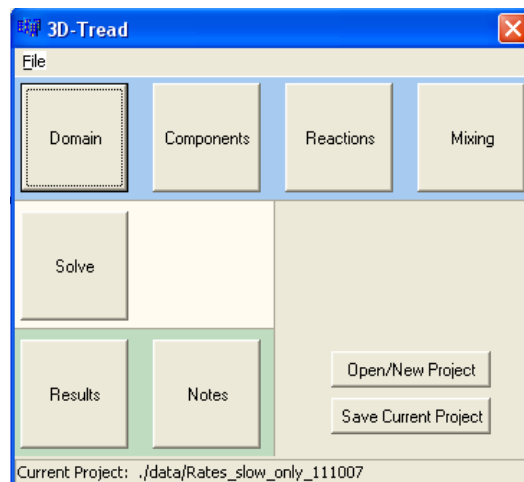
Figure 1. The main menu – graphical user interface (GUI) for the 3D-TREAD model.

4. Loading the GUI

To start using the model run the executable file (sediment3d.exe). A folders/files dialogue box will appear whenever the model is started, allowing loading of a saved model. The path to the data folder will need to be set at the first use of the model ((place installed)/3DTREAD/data). Whenever the model is executed either, a previous file can be loaded, or a filename for a new model can be entered. Filenames must not contain any spaces. Once the name is set, or a saved model is selected, only the main menu will be shown. The active projects filename is shown at the base of this menu.

5. Input parameters

Each button along the top line of boxes in the main menu, opens up additional interface boxes for entering of specific parameters (domain, components, or reactions; the mixing functionality is currently under development and is not explained here).

5.1. Domain and porosity inputs

Figure 2 show the graphical interface for these input parameters, which can be opened by pressing the 'Domain' button in the main menu. The porosity profile setting box can be opened by pressing the 'Porosity profile' box in the 'Domain' box.
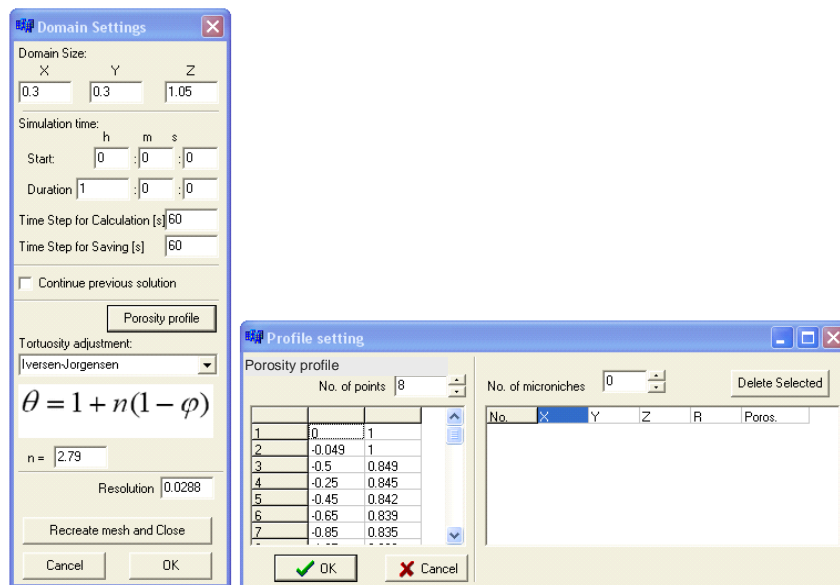
Figure 2. Domain and porosity input interfaces.

X, Y and Z, are the domain dimensions in cm. Typically, to obtain optimum results in minimal time a 'pencil' type approach to the domain shape has been used (e.g. x and y = 0.3, z = 1 cm). Duration is the length of time over which the simulation is required, numbers should be entered here as integers (start time has no effect on the simulation and can be ignored). 'Time Step for Calculation' allows specification of the interval

between each calculation (in s). 'Time Step for Saving' (s) allows the user to specify how often the output from the stepwise calculations are written to the output file. The value must be equal or greater than the calculation time step. It is crucial that these values are set to ensure that the last calculation of the model run is saved to the output files (e.g. specifying a 55 s runtime but a 10 s calculation time will result in the output being unreadable due to the lack of final values).

Several pre-set options are available for the specification of tortuosity-porosity relationships, including allowing user setting of the equation variables. For further details see Sochaczewski et al (2008) or the sources used; Boudreau (1997), and Boudreau and Meysman (2006). Porosity is entered as finite values in 3D TREAD not as equations. The user can specify any number of depth coordinates and the associated porosities as a list. For microniches the porosity should be specified as a single value, along with the coordinates and radius.

Resolution controls the density of the 3D mesh and thus the spatial resolution of the simulations. Lower resolutions will tend to result in niches with shallower concentration gradients at the niche edge. Setting too high a resolution will result is several problems: the node limitations of the software may be exceeded and the model will not run; the output file may become too large for Matlab to extract the data; or the simulation run-time will be greatly extended. As a rule of the thumb the maximum resolution can be set at: approximately the cube root of the domain volume ($\sqrt[3]{(x \times y \times z)}$) divided by 15. Actual achievable resolution will depend upon the processing power of the computer and this estimate is only a guide.

5.2. Components input

Figure 3 shows the input interfaces for the modelled components.
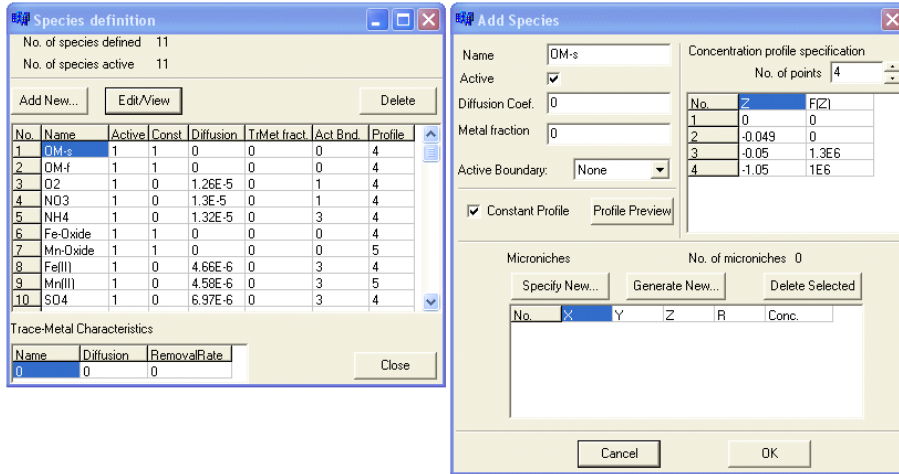
Figure 3. Component input interface boxes.

By selecting the 'Add New…' button the 'Add Species' box is opened. Using this interface all of the component properties can be entered. The species name should not contain spaces. Diffusion coefficients should be entered in $cm^2 \, s^{-1}$. The 1D profiles for the component outside of the niche are entered by specifying a chosen number of points, and associated concentrations, throughout the z domain (depth coordinates should be specified as negative values and this rule applies to any depth specification throughout the model parameterisation). For microniches, the coordinates, radius and the concentration are required (microniche values are applied independently in the mesh specification and therefore zones of lower or higher concentration can be modelled for microniches). Boundaries can be specified as: only upper or lower, both, or no active boundary. Where boundaries are specified these are assumed to be fixed concentration (Dirichlet) boundaries and values are taken from the user specified concentration profiles. Where no boundaries are specified they are assumed to have a zero concentration gradient.

If an assumption of steady state is required to be applied to a component concentration, the 'Constant Profile' option can be selected. Using this option the concentrations are reset as the user specified initial conditions after each calculation time-step. (The 'Trace-Metal Characteristics,' 'Active' and 'Metal fraction' inputs are remnants of earlier versions and can be ignored). Once the species have been added, diffusion coefficients can be edited directly from the 'Species definition' interface, all other parameters can be edited using the 'Edit/View' button.

5.3. Reactions input

Figure 4 shows the input interface for specifying reaction stoichiometry and associated data for the modelled components.
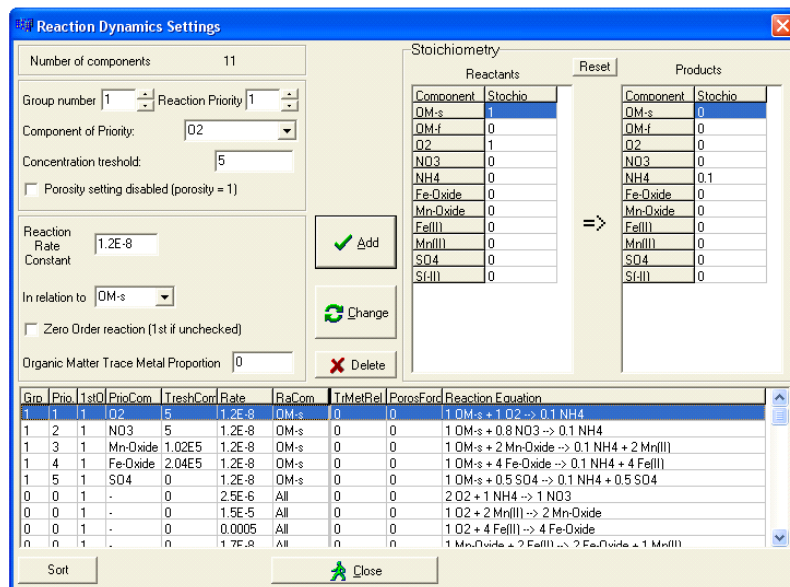

Figure 4. Reactions input interface boxes.

All the reactive species can participate in reactions that each have a set of user-specified values.

- Priority group number and reaction priority within this group. Organic matter fractions are typically given group numbers of 1, 2, etc., with the 'Reaction

Priority' set according to the order of utilisation of the electron acceptors ($O_2 = 1$, $NO_3^- = 2$ etc.). Secondary reactions are typically given a group and priority of 0.

- For OM reactions reference component (oxidant) and the associated concentration threshold should be specified. (The 'Organic Matter Trace Metal Proportion' function is not active and can be ignored).

- Reaction rate constants for all reactions, with specification to which reactant it is related – i.e. OM in case of OM decomposition reactions, or all components for secondary reactions.

- Type of reaction kinetics (zero or first order).

- Chemical equation of the reaction (stoichiometric values).

Once all of the values for an individual reaction have been entered they can be saved by clicking the 'Add' button. To edit a reaction, highlight it in the list, make the required changes and save by clicking the 'Change' button. To create a new reaction similar to one that has been saved, select that reaction, make the required changes then click the 'Add' button.


6. Running a simulation

If the model is not to be run immediately the data can be saved manually by clicking the 'Save Current Project' button on the main menu. Otherwise, once all of the input and domain data have been entered clicking the 'Solve' button will automatically save all of the parameters to the appropriate files, hide the menu, and open a 'DOS – type' screen showing the progress of the model run. Once the run is complete the main menu will reappear and the results can be extracted. If an error message 'Solver Crash!!! Check Parameters' displays soon after clicking the 'Solve' button there may be parameters missing or the mesh density may be too high.

Continuing a previous solution

If a model run requires a longer simulation than initially programmed it is not necessary to rerun the entire simulation. In the 'Domain' interface the 'Continue previous solution' box can be checked and the final solution concentration values for the previous solution will be applied as the initial model values. The run time ('Duration') can be altered before running the model. The mesh must be consistent, therefore the X, Y, Z and resolution parameters must not be changed. Once 'Solve' is pressed the previous results file will be overwritten. <u>Therefore, all result extraction from the initial run must be performed before using this procedure.</u>

7. *The output file and extracting data*

Before using the 'Results' interface it is necessary to run Matlab and change the 'Current Directory' pathway to the 3D TREAD folder. Figure 5 shows the interface for selection of results for output and display. Plots can be set for either the x or y planes (versus depth – z).
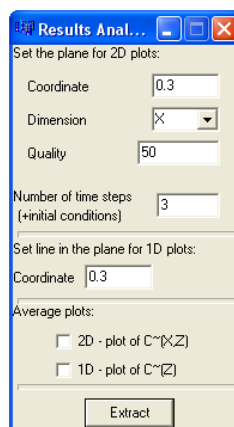
Figure 5. Interface for selection of required output.

The coordinate set for the 2D plot will determine the location of the 2D plane. Combined with the 2D value, the coordinate for the 1D plot gives the x, y location of

the line plot. 'Quality' sets the number of coordinate plotted for each axis (maximum value of 256). For example if z is 1 cm long and the 'Quality' is set at 51 then the 1D plot will have data points at 0.2 mm intervals. The initial conditions are automatically plotted; the user can select how many, if any, intermediate time-steps are plotted (selecting a value of 1 for the 'Number of time steps' will only plot the final values; values greater than one will result in plots for values at intermediate time-steps). The 'Average plots' functions can be ignored. Once the values have been set, press the 'Extract' button. Then in Matlab run the 'plotresults.m' file (right click, then select 'run'). Matlab will generate a figure for each specified components. Each figure will contain both the 1D and 2D plots. As well as the figures, Matlab will also create a CSV file of all of the 1D plots for each component based upon the 'Quality' and 'Number of time steps' values. This file will be saved to the 'data' folder with the same filename as specified for the model run. If results are required for several coordinates for the same model run it is necessary to change the name of this file after each run, as otherwise it will be overwritten each time the results are extracted for a given model run.

8. Creating new input files from existing files

Instruction on how to create an new input file from an existing file. 1) Run the .exe file and open the existing file. 2) Click the 'Open/New Project' button. 3) Enter the required new filename. 4) Click 'Save' 5) Click 'Save Current Project'. 6) Open the 'Domain' box and click the 'Recreate mesh and Close' button (this creates a correctly named mesh file). The new file is ready and can be altered as required. <u>If species need to be removed it is best to create a brand new file rather than using this procedure, this avoids problem with the species changing within specified reactions.</u>

9. Supplementary information

Known issues

After successful completion of some model runs (often for simulations with short runtimes, or where coarse mesh domains are used) an error message is shown. This message contains the text 'The exception unknown software exception (0xc0000005) occurred in the application at location 0x00448e7e.' Once this error box has been closed, a second error will be displayed 'Solver Crash!!! Check Parameters.' However, the model will have completed successfully in this case and the results can be extracted as normal.

File extensions

Several files are created by the model to specify input parameters and output data. Table 1 shows the file extensions used by 3D TREAD for saving model input and output data. In addition to these files the file 'setup.d' contains the results interface parameters for only the most recently used file.

Table 1. File extensions used by 3D TREAD for model input and output data.

File extension	Stored values
domain.m	Mesh specification
.prj	All inputs entered in the 'domain inputs' box
micro.par	Programme remnant, necessary for model to run but contains no input data
rates.par	All reaction dynamics settings (stoichiometry, rates, etc..)
spec.par	A list file names for all specified components
spec_NAME.par	Name and parameters specified for each component (where NAME is the component name specified by the user)
!results.out	Model output for each component at each saved time step for the entire mesh
!results.out.cont	Component concentrations for the entire mesh for the end of the simulation only, allows these conditions to be applied to a continued model run
!results_plots.csv	Created by Matlab when the results are plotted, contains 1D data for each component and time-step based on user specified output requirements
stats.txt	Records the model runtime after the simulation is complete

10. Future Updates

The following updates are planned or underway:

- Removal of non-essential (legacy) functions

- A function allowing specification of precipitation reactions for e.g. sulphides

- Defining high mesh resolution at microniche edges

- Plotting of data across the z axis

- Addition of a function allowing exponential growth for reaction rates

- A built in plotting function, removing the need for Matlab

11. Further information

For additional information, including copies of the 3D TREAD manuscript(s), contact

Prof. Bill Davison,
Environmental Science Department,
Lancaster Environment Centre,
Lancaster University,
Lancaster LA1 4YQ
UK

E-mail: w.davison@lancaster.ac.uk
Fax: +44 (0)1524 593985

Appendix C

Typical treatment of iron – sulphide reactions

Typically, modelled iron sulphide precipitation/dissolution reactions are assumed to follow Equation 1 (e.g. Boudreau, 1996; also often shown in a simplified form where bicarbonate and carbon dioxide are excluded).

$$Fe^{2+} + HCO_3^- + HS^- \underset{r_{diss}}{\overset{r_{pptn}}{\rightleftarrows}} FeS + CO_2 + H_2O \qquad (1)$$
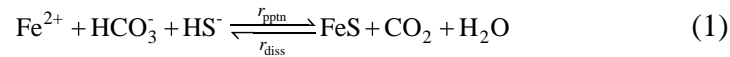
The empirical rate laws stated in Wang and van Cappellen (1996) are show as Equations 2, 3 and 4. [FeS] is a proxy for the surface area and is excluded from Equation 2, as there may be no initial solid phase (see van Cappellen et al, 1993).

$$r_{pptn} = k_{pptn}\delta_{pptn}(\Omega_{FeS} - 1) \qquad (2)$$

$$r_{diss} = k_{diss}\delta_{diss}[FeS](1 - \Omega_{FeS}) \qquad (3)$$

where:

$$\Omega_{FeS} = \frac{[Fe^{2+}][HS^-]}{\{H^+\} K'_{FeS}} \quad \begin{array}{ll} >1: \delta_{pptn} = 1 & \delta_{diss} = 0 \\ \leq 1: \delta_{pptn} = 0 & \delta_{diss} = 1 \end{array} \qquad (4)$$

This relationship is widely used in diagenetic models (e.g. Wijsman et al, 2002; Morse and Eldridge, 2007). In applying this approach δ acts as a simple switch that only allows either the forward or reverse reaction to proceed.